Department of Biotechnology and Chemical Technology

Phase Equilibrium Measurements and Modelling for Separation Process Design

Claudia Dell'Era

Aalto University

DOCTORAL DISSERTATIONS

Aalto University publication series
DOCTORAL DISSERTATIONS 20/2012

Phase Equilibrium Measurements and Modelling for Separation Process Design

Claudia Dell'Era

Doctoral dissertation for the degree of Doctor of Science in Technology to be presented with due permission of the School of Chemical Technology for public examination and debate in Auditorium KE2 (Komppa Auditorium) at Aalto University School of Chemical Technology (Espoo, Finland) on the 16th of March, 2012, at 12 noon.

Aalto University
School of Chemical Technology
Department of Biotechnology and Chemical Technology
Research group of Chemical Engineering

Supervisor
Professor Ville Alopaeus

Instructor
Dr. Juhani Aittamaa

Preliminary examiners
Associate Professor Kaj Thomsen. Technical University of Denmark, Denmark

Prof. Dr. -Ing. Hans Hasse. University of Kaiserslautern, Germany

Opponent
Prof.dr.ir Cornelis J. (Cor) Peters. Petroleum Institute, United Arab Emirates

Aalto University publication series
DOCTORAL DISSERTATIONS 20/2012

ISBN 978-952-60-4518-4 (printed)
ISBN 978-952-60-4519-1 (pdf)
ISSN-L 1799-4934
ISSN 1799-4934 (printed)
ISSN 1799-4942 (pdf)

Unigrafia Oy
Helsinki 2012

Finland

The dissertation can be read at http://lib.tkk.fi/Diss/

441 697
Printed matter

Author
Claudia Dell'Era

Name of the doctoral dissertation
Phase Equilibrium Measurements and Modelling for Separation Process Design

Publisher School of Chemical Technology

Unit Department of Biotechnology and Chemical Technology

Series Aalto University publication series DOCTORAL DISSERTATIONS 20/2012

Field of research Chemical Engineering

Manuscript submitted 20 September 2011 **Manuscript revised** 13 December 2011

Date of the defence 16 March 2012 **Language** English

☐ **Monograph** ☒ **Article dissertation (summary + original articles)**

Abstract

The purpose of this research was to develop modelling of industrial processes by improving the thermodynamic representation of the equilibrium between phases. For this purpose an extensive experimental work was performed, comprising of vapour-liquid, gas-liquid and solid-liquid equilibrium measurements.

Vapour liquid equilibrium of binary mixtures of butane + alcohols was measured with a static total pressure apparatus due to the importance of hydrocarbon and alcohol mixtures in the production of biofuels. The same equipment was used to measure binary systems of diethyl sulphide + C4 – hydrocarbons of importance in refinery applications. The activity coefficients of these systems were modelled with activity coefficients models.

The absorption of carbon dioxide in alkanolamine solutions is the leading technology for the removal of carbon dioxide during refining of gas and oil. In recent years, this technology has gained importance also for carbon capture from large point sources. The scarcity of experimental data for some alkanolamine systems affected the accuracy of thermodynamic models. Several experimental techniques were developed to supply new experimental data for aqueous solutions of diisopropanolamine (DIPA) and methyldiethanolamine (MDEA). The solubility of carbon dioxide in solutions of these amines was measured with a static total pressure apparatus for gas solubility, and with a bubbling apparatus. The density of carbonated aqueous DIPA was also measured and modelled. The vapour-liquid equilibrium of water + DIPA and water + MDEA was measured with a static total pressure apparatus. The solid-liquid equilibrium of the same systems was measured with a visual method and a Differential Scanning Calorimeter. The activity coefficients of aqueous DIPA and MDEA solutions were modelled using NRTL, thus providing the first model of this sort for DIPA. A new model of the Henry's law constant of carbon dioxide in binary and ternary aqueous solutions of alkanolamines was developed at temperatures up to 393 K.

Keywords vapour-liquid equilibrium, solid-liquid equilibrium, solubility, carbon dioxide, DIPA, MDEA, butane, diethyl sulphide, UNIFAC, COSMO, Henry's law, miniplant

ISBN (printed) 978-952-60-4518-4 **ISBN (pdf)** 978-952-60-4519-1

ISSN-L 1799-4934 **ISSN (printed)** 1799-4934 **ISSN (pdf)** 1799-4942

Location of publisher Espoo **Location of printing** Helsinki **Year** 2012

Pages 128 **The dissertation can be read at** http://lib.tkk.fi/Diss/

Preface

The research work presented in this thesis was completed during the years 2004 -2007 and 2009-2011 at the Chemical Engineering research unit of Aalto University School of Chemical Technology (operating as Helsinki University of Technology until 2009).

Fortum Foundation is acknowledged for their economic support, in the form of a 4 years scholarship from 2004 to 2007.

My professor Ville Alopaeus and my former professor Juhani Aittamaa receive my gratitude for their guidance and support during all these years. My thanks also go to Dr. Kari I. Keskinen, who proposed the subject and supported me in obtaining funding for this research.

Warm thanks are due to my co-author, guide and friend Dr. Petri Uusi-Kyyny. He taught me how experimental research is conducted, he helped me overcoming practical and theoretical problems and he was always a valuable support, both technologically and humanly. I will never forget the importance of his contribution to this research and to my growth as a chemical engineer and scientist.

I wish to express my gratitude to all my co-authors; it was a great pleasure to work with every one of you. In particular, I would like to acknowledge Dr. Juha-Pekka Pokki for his help in addressing difficulties with thermodynamic modelling and Dr. Kaj Jakobsson for supporting me with computation and programming. I wish also to separately thank Anne Penttilä, with whom I worked intensely in the last two years.

The working environment within the Chemical Engineering research unit was always creative, inspiring and friendly. Therefore, I would like to thank all my former colleagues for their contributions and in particular my friends Anna Zaytseva, Erlin Sapei and Raisa Vermasvuori. During these years as a researcher I also meet two of my best friends, Asta Nurmela and Piia Haimi. I wish to thank them dearly for their unconditioned support, for the liberating conversations and for all fun and laughter! With their love and patience, they contributed to making Finland my new home.

From the personnel of the Chemical Engineering research unit, I would also like to thank Sirpa Aaltonen and Lasse Westerlund who helped throughout the years in dealing with practical issues and who always had a nice word for me.

My mum Lucia, my dad Angelo and my brother Enrico deserve my deepest gratitude. Even if we live in different countries, they fight the distance to make me feel the warmth of their love and support.

This thesis is dedicated to my husband Daniel and my son Robin, whom I deeply love. I wish to thank them for bringing joy and meaning to my life.

Claudia Dell'Era Espoo, 22nd January 2012

List of publications

I. Penttilä, A., **Dell'Era, C**., Uusi-Kyyny, P.; Alopaeus, V. The Henry's Law Constant of N_2O and CO_2 in Aqueous Binary and Ternary Amine Solutions (MEA, DEA, DIPA, MDEA, and AMP)**.** Fluid Phase Equilibria 311 (2011) 59–66.

II. **Dell'Era, C**., Uusi-Kyyny, P.,Rautama, E.-L., Pakkanen, M., Alopaeus, V. Thermodynamics of aqueous solutions of methyldiethanolamine and diisopropanolamine. Fluid Phase Equilibria 299 (2010) 51–59.

III. **Dell'Era, C**., Uusi-Kyyny, P., Pokki, J.-P., Pakkanen, M., Alopaeus, V. Solubility of carbon dioxide in aqueous solutions of diisopropanolamine and methyldiethanolamine. Fluid Phase Equilibria 293 (2010) 101–109.

IV. **Dell'Era, C**., Pokki, J.-P., Uusi-Kyyny, P., Pakkanen, M., Alopaeus, V. Vapour-liquid equilibrium for the systems diethyl sulphide + 1-butene, + cis-2-butene, + 2-methylpropane, + 2-methylpropene, + n-butane, + trans-2-butene, Fluid Phase Equilib. 291 (2010) 180-187.

V. **Dell'Era, C**., Zaytseva, A., Uusi-Kyyny, P., Pokki, J.-P., Pakkanen, M., Aittamaa, J. Vapour-liquid equilibrium for the systems butane + methanol, +2-propanol, +1-butanol, +2-butanol, +2-methyl-2-propanol at 364.5 K, Fluid Phase Equilib., 254 (2007) 49-59.

VI. Ouni, T., Lievo, P., Uusi-Kyyny, P., **Dell'Era, C.**, Jakobsson, K., Pyhälahti, A., Aittamaa, J. Practical Methodology for Distillation Design using Miniplant. Chem. Eng. Tech. 29 (2006) 104-112.

Statement of the author's contribution to the appended publications

I. The author supervised the work, contributed to the development of the model, and helped in writing the manuscript.

II. The author designed and set-up the experimental measurement systems with co-author Uusi-Kyyny. The author conducted most of the experimental work, analysed the results, modelled the systems and wrote the paper.

III. The author designed and set-up the experimental measurement systems with co-author Uusi-Kyyny. The author conducted most of the experimental work, analysed the results and wrote the paper.

IV. The author analysed the results, modelled the systems and wrote the paper.

V. The author analysed the results, modelled the systems and wrote the paper.

VI. The author developed the model of the column, and contributed to writing the manuscript in relation to the column model.

Notations

Symbols

a	attractive parameter of the Soave-Redlich-Kwong equation of state
a_{ij}	interaction parameters of the NRTL model
A	fitted parameter of activity coefficient model
A_{ij}	parameter of the Henry's law constant model for solvent components ij
A_{ijk}	parameter of the Henry's law constant model for solvent components ijk
b	co-volume parameter of the Soave-Redlich-Kwong equation of state
b_i	co-volume parameter of the Soave-Redlich-Kwong equation of state for component i
b_{ij}	interaction parameters of the NRTL model
B_{ij}	parameter of the Henry's law constant model for solvent components ij
B_{ijk}	parameter of the Henry's law constant model for solvent components ijk
C_{ij}	parameter of the Henry's law constant model for solvent components ij
C_{ijk}	parameter of the Henry's law constant model for solvent components ijk
c_p	heat capacity
D_{ij}	parameter of the Henry's law constant model for for solvent components ij
f	fugacity
G	Gibbs energy
g_{ij}	interaction parameters of the NRTL model
$H_{i,j}$	Henry's law constant of solute i in solvent component j
$H_{i,jk}$	Henry's law constant of solute i in a solution of j and k
$H_{i,jkm}$	Henry's law constant of solute i in a solution of j, k and m
H	enthalpy
$\Delta H_{i,fus}$	enthalpy of fusion of component i
k_{ij}	interaction parameter of the Soave-Redlich-Kwong equation of state
N	number of components
N_P	number of experimental points
P	pressure
P_i	partial pressure of component i
P_i^{sat}	vapour pressure of pure component i
q	calculated variable
R	ideal gas constant
s	measured variable
T	temperature
u	measured variable
V	volume
V_i	molar volume of component i

w_i	weight fraction
$wt\%$	weight percent
x	mole fraction
Z	compressibility factor

Greek letters

α	loading = moles of absorbed CO_2 / moles of amine
α_{SRK}	parameter of the Soave-Redlich-Kwong equation of state
α_{ij}	non-randomness parameter of the NRTL and e-NRTL models
δ	uncertainty
Φ	volume fraction
Δ	difference
ϕ	fugacity coefficient
γ	activity coefficient
ρ	density
τ_{ij}	interaction parameters of the NRTL model and e-NRTL models
ω	acentric factor (Soave-Redlich-Kwong equation of state

Superscripts

α	phase
β	phase
EX	excess
L	liquid
S	solid
Sat	saturated
V	vapour
$\bar{q}$	partial property (q)
∞	infinite dilution
$*$	unsymmetric convention
^{o}	pure component (standard state)
^	mixture
-	minimum value
+	maximum value
q'	perturbed value (of q)

Subscripts

$calc$	calculated
exp	experimental
fus	fusion
i	component
j	component
k	component
l	experimental point

m	component
S	solvent
tp	triple point
W	water

Abbreviations

AMP	2-amino-2-methyl-1-propanol
atm.	atmospheric (pressure)
DEA	diethanolamine
DES	diethyl sulphide
DGA	2-(2-aminoethoxy) ethanol
DIPA	diisopropanolamine
DSC	differential scanning calorimeter
EOS	equation of state
FCC	fluid catalytic cracking
GLE	gas-liquid equilibrium
HETP	height equivalent to a theoretical plate
LPG	liquefied petroleum gas
MDEA	methyldiethanolamine
MEA	monoethanolamine
MTBE	methyl *tert*-butyl ether (2-methoxy-2-methyl propane)
PVT	pressure-volume-temperature
RK	Redlich-Kwong equation of state
SLE	solid-liquid equilibrium
SRK	Soave-Redlich-Kwong equation of state
TEA	triethanolamine
VLE	vapour-liquid equilibrium

Table of contents

1 Introduction

Mathematical models are powerful tools in the development and design of chemical units. Process design is usually performed by constructing a mathematical model of the entire process. Various design options may then be evaluated quickly and inexpensively at an early stage of the design process. Commonly, a pilot plant is built to provide design and operating information before the construction of a large plant. Scale-up methods are applied to extrapolate the pilot plant up to full scale. The construction of several plants of intermediate size may be necessary if simple scale-up rules are applied, since they usually do not allow large size extrapolation steps. The construction of pilot plants is costly and time demanding. Strengthening model-based process design is the most efficient way of reducing the need of pilot plants. Particularly in the case of separation units, an accurate mathematical representation of the process phenomena might be sufficient to design full scale chemical plants.

Various phenomena take place in chemical units, such as phase equilibrium, mass and heat transfer, chemical reactions and hydraulics. An accurate description of these phenomena can only be achieved with the aid of good quality experimental data. In separation processes, the formation or co-existence of different phases is exploited in order to separate the compounds of interest. A model of the thermodynamic equilibrium between phases provides the basis for successfully designing these chemical units. Thermodynamic is composed of mathematical equations derived from very few fundamental postulates [1]. A general thermodynamic model is applied to a specific process using physical properties at the operative conditions of interest. It was the aim of this work to improve thermodynamic modelling of separation unit for chosen systems of industrial interest. For these systems, phase equilibrium data were either scarce or unavailable in the open literature. An extensive experimental work was performed to supply vapour-liquid equilibrium (VLE), solid-liquid equilibrium (SLE) or gas solubility (GLE) data. In addition, the systems studied were described either with traditional thermodynamic models or with new expressions.

In absence of experimental data, phase equilibrium can also be predicted. The accuracy of predictive models is often inadequate for modelling chemical units that are sensitive to

phase equilibrium, e.g. reactive distillation. In this work, the performances of some predictive methods on selected systems of interest were investigated.

1.1 The miniplant concept

Model-based process design has the great advantage of being inexpensive and versatile. On the other end, process design using pilot plants and scale-up is a robust way to proceed. The greatest danger in model-based design is that some important factor may go unnoticed during design. This rarely happens when pilot plants are used, since all aspects of plant design and operation are encountered during the scale-up process.

The miniplant concept is a compromise solution between the two approaches. Design using a miniplant is mostly achieved through model-based process design. A small scale pilot plant, i.e. the miniplant, is then constructed, and the performances of the model are tested against experimental runs. In comparison to a traditional pilot plant, a miniplant has a smaller scale, thus reducing utility costs and risks related to operation safety.

In this work, a miniplant was used to test the performances of the thermodynamic models used in designing distillation columns [VI]. The industrial column of interest was part of a process for producing isooctane from isobutylene (NExOCTANE, Figure 1.1 [2]). In the NExOCTANE process, isobutylene is dimerized to isooctane in a reactor. Water and 2-methyl-2-propanol are used as inhibitors to the formation of larger chain oligomers of isobutene in the reactor. The distillation column separates isooctene from the aqueous mixture containing 2-methyl-2-propanol and short-chain hydrocarbons. Isooctene is then hydrogenated to isooctane, which may be used instead of MTBE (methyl-*tert*-butyl ether) to increase the octane number in petrol [VI].

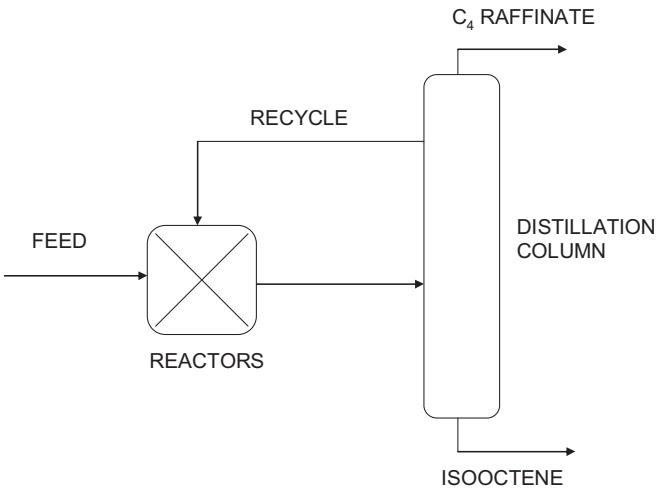

Figure 1.1 Schematic representation of the NExOCTANE process.

1.2 Systems of interest

The vapour-liquid equilibrium of mixtures of alcohols and hydrocarbons is important for process design and optimisation in the field of biofuels. Methanol, ethanol and butanol are among the fuels produced by gasification of biomass, cracking or fermentation. Alcohols are widely used also in the oil industry, e.g. as fuel additives and inhibitors [3]. In particular, the VLE of binary systems of 2-methyl-2-propanol + hydrocarbons is needed in modelling the production of isooctane from isobutylene with the NExOCTANE [2] process, in which 2-methyl-2-propanol is used as inhibitor.

The VLE of solutions of butane and methanol is of particular interest due to the azeotrope formed by the combination of a polar and a non-polar compound. In addition, the tendency to self-associate evidenced by the molecules of methanol makes the behaviour of the mixture strongly non-ideal [4]. For these reasons several researcher groups measured the vapour-liquid equilibrium of butane + methanol at various temperatures [4-10]. A great amount of data is necessary to successfully model this complex system and to determine the position of the azeotrope. Therefore, the VLE of butane + methanol was measured in this work at 364.5 K [V]. At the same temperature were measured binary VLE data for the systems of butane + 2-propanol, + 1-butanol, + 2-butanol, + 2-methyl-2-propanol [V]. Our research group also measured binary VLE data of butane with

methanol, 2-propanol, 2-butanol and 2-methyl-2-propanol at 323 K [11]. Kretschmer and Wiebe [5] published some equilibrium data points for the system of n-butane + 2-propanol at temperatures lower than 364.5 K. The VLE of butane + 1-butanol was measured by Deák et al. [12] at various temperatures. Isobaric VLE measurements of butane + 2-butanol were found at 0.5 and 0.7 MPa in the temperature range from 320 to 440 K [13]. Melpolder [14] measured at various temperatures the VLE of butane + 2-methyl-2-propanol.

Vapour-liquid equilibrium data of sulphur compounds in hydrocarbons are of great interest for the oil industry. Sulphur compounds are present in raw oil or produced during refining. Due to the detrimental environmental effect of many sulphur compounds, their amount in fuels is strictly regulated. Refineries face the challenge of designing units capable of removing sulphur compounds down to trace levels in order to comply with regulations. The greatest amount of sulphur in fuels comes from petrol produced by fluid catalytic cracking (FCC) mainly in the form of thiols, sulphides and thiophenes [15, 16]. Diethyl sulphide (DES) is formed in the FCC units through chemical reactions from sulphur compounds present in the feedstock [16, 17]. The VLE of the systems of diethyl sulphide in C_4-hydrocarbons, i.e. 1-butene, cis-2-butene, 2-methylpropane, 2-methylpropene, n-butane and trans-2-butene, was measured in this work [IV]. No VLE data were found in the open literature for any of the measured systems. Extensive work was conducted in our research group on the VLE of DES in hydrocarbons by Sapei et al. [18-21].

Carbon dioxide is present in great quantity in gas streams, LPGs and crudes, alongside sulphur compounds, which occur in widely varying amount depending on the crude. Many sulphur compounds are removed from hydrocarbons by converting them into hydrogen sulphide by reaction with hydrogen in presence of a catalyst. As a consequence, the gas streams produced during refining contain a substantial amount of hydrogen sulphide, an extremely poisonous and corrosive gas [22].

In the oil industry, chemical absorption of CO_2 and H_2S, both acidic gases in aqueous solutions, is traditionally carried out in an absorber unit by means of a regenerable solvent. Aqueous solutions of alkanolamines are used as solvents, being weak bases that react reversibly with these contaminants [22]. In the absorber unit, the acid gas stream is

contacted counter-currently with the amine solution, and the acid impurities are absorbed into the solvent. The amine solution is then regenerated by reversing the chemical reactions with the help of lower pressure and higher temperature conditions. The regenerated solvent solution is returned to the absorber [22, 23].

Recently, carbon dioxide has received great attention for its role as a greenhouse gas. The capture and subsequent storage of carbon dioxide from large point sources is explored as a possible technical solution in limiting the amount of carbon dioxide released to the atmosphere. Renewed interest towards alkanolamines as CO_2 absorbents has grown along with the possibility of adapting traditional gas sweetening technologies to carbon capture. Good knowledge of the behaviour of CO_2 in aqueous alkanolamines solutions is essential to adjust the traditional alkanolamine technology to this new function.

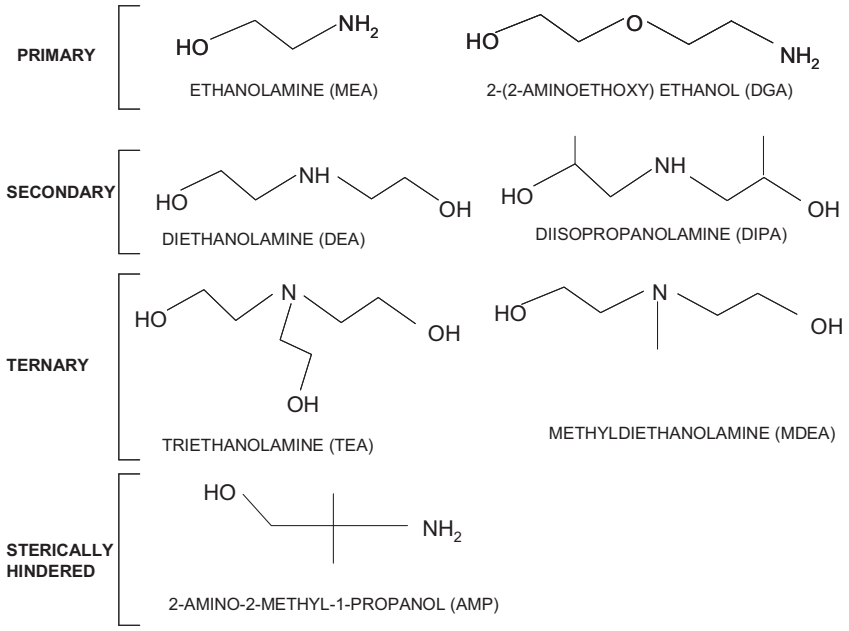

Figure 1.2 Structural formulas of commonly used alkanolamines.

A broad variety of alkanolamines is used for the absorption of carbon dioxide and hydrogen sulphide. Monoethanolamine (MEA) and 2-(2-aminoethoxy) ethanol (DGA) are primary amines, i.e. they have two hydrogen atoms directly attached to a nitrogen atom, and they are the most alkaline. Secondary amines are diethanolamine (DEA) and

diisopropanolamine (DIPA) and ternary amines are triethanolamine (TEA) and methyldiethanolamine (MDEA) [23]. Sterically hindered amines are also employed in gas sweetening, in particular 2-amino-2-methyl-1-propanol (AMP). MEA and DEA are traditionally the most used amines. However, highly concentrated MEA solutions are avoided in presence of CO_2 due to their high aggressiveness towards materials. DEA forms carbamates when reacting with CO_2, therefore its absorption capabilities are reduced [24]. MDEA is known as a high-capacity selective solvent for H_2S in presence of CO_2. The use of amine blends, in particular blends of MDEA with primary amines such as MEA or AMP, has improved the absorption of MDEA with respect to CO_2 [23, 24]. DIPA is primarily utilised in Europe as the solvent amine in the Adip solution of the Shell Adip process [23]. Even though DIPA has been used for a long time in gas sweetening, there are relatively few experimental data on aqueous solutions of DIPA in the open literature. This scarcity of data reflects on the quality of the thermodynamic models of systems containing DIPA. Thus, among the amines, DIPA was the primary interest of this research.

In this work, the solubility of CO_2 in water + DIPA was measured with two experimental techniques at various temperatures and compositions of the solvent [III]. Solubility data of CO_2 in water + DIPA were found in Isaacs et al. [25] and in ter Maat et al. [26]. Great attention was also given to MDEA for its importance in new applications, such as carbon capture units. The solubility of CO_2 in water + MDEA was measured at various temperatures and solvent compositions. The solubility of CO_2 in water + MDEA was investigated by many research groups at various conditions of temperature and composition. For this reason, MDEA was also used for validating some of the experimental techniques developed in this research. In [27-34] were found some data point at similar experimental conditions than those studied in this work [III].

The thermodynamics of the solvent solutions, i.e. water + alkanolamine, strongly influences the solubility of CO_2, especially at low gas loadings. SLE data are the most appropriate to calculate the activity coefficients of aqueous alkanolamine solutions at low amine concentrations. For water + alkanolamine systems, VLE data are valuable mainly at high temperature and at high amine concentrations [35].This limitation is caused by the high difference in boiling point and vapour pressure of the system compounds. In this

work, the VLE and SLE of water + DIPA and water + MDEA were measured [II]. In particular, the investigation of VLE data focused on the experimental conditions of significance for water + alkanolamine systems. The activity coefficients of these solutions were modelled using the NRTL [36] model, which is particularly suitable for aqueous systems [37].

Neither VLE nor SLE data of water + DIPA were found in the literature. Only Long and Yamin [38] published a model for the activity coefficients of this system in the journal of their university. They fitted the empirical parameters of the NRTL model against their own VLE measurements, but these data are not given in tabulated form in their article. In this work, the activity coefficients of water + DIPA were modelled using the measured VLE and SLE data [II], thus proposing the first model of this sort for water + DIPA.

VLE data points of water + MDEA were available from several sources at low amine concentrations [39-43]. In this work, VLE measurements were mainly conducted at high amine concentrations, where VLE data are sufficiently accurate for activity coefficients modelling. With the exception of Kuwairi [39] and Xu et al. [42], who specifically studied the vapour pressure of aqueous MDEA solutions, the other data points were the solvent vapour pressures measured during gas solubility investigations. The SLE of water + MDEA was measured by Chang et al. [35]. After the publication of our work [II] also Fosboel et al. [44] published SLE data for the system of water + MDEA. Several models of the activity coefficients of water + MDEA were found in the literature, all of them using the NRTL equations. The regressions of the model parameters were based either solely on VLE data [45], on VLE and SLE data [35], or on VLE, SLE and excess enthalpy data [46-48]. In this work, the activity coefficients of water + MDEA were modelled using VLE, SLE and excess enthalpy data [II].

It was noticed that many literature models of the Henry's law constant of CO_2 in aqueous solutions of alkanolamines deviated at high temperatures from the experimental measurements. This is a source of error in describing the solubility of CO_2 in these solvents. Therefore, a model of the Henry's law constant of CO_2 in aqueous solutions of alkanolamines, and alkanolamine blends was developed [I]. The performances and strengths of this model were evidenced by comparison with similar models found in the literature [49-55].

A comprehensive thermodynamic model of the solubility of CO_2 in alkanolamine solutions can be developed in the future, based on the achievements of this research work. In fact, after the publication of [II] and [III] Zong et al. [56] used this work to extend their CO_2 solubility model to aqueous solutions of DIPA, thus confirming the importance of these data in the development of thermodynamic modelling of alkanolamine solutions.

2 *Thermodynamic principles*

2.1 Phase-equilibrium thermodynamic

Phase-equilibrium thermodynamic describes the equilibrium distribution of the components among the phases present in the system [57]. Phase-equilibrium thermodynamic is extensively treated in [1, 37, 57, 58]. A short summary is here presented, with focus on the equations used in this work.

For any species *i* in a mixture, the condition of thermodynamic equilibrium between two phases α and β can be written in terms of fugacities as in:

Eq. 2.1 $$\hat{f}_i^{\alpha} = \hat{f}_i^{\beta}$$

2.1.1 Vapour-liquid equilibrium (VLE)

In the case of VLE, Eq. 2.1 becomes:

Eq. 2.2 $$\hat{f}_i^{V} = \hat{f}_i^{L}$$

The fugacity of component *i* in vapour phase is expressed in terms of fugacity coefficients $\hat{\phi}_i^{V}$ according to:

Eq. 2.3 $$\hat{f}_i^{V} = x_i^{V} \hat{\phi}_i^{V} P$$

Equivalently, the fugacity of a component *i* in liquid phase can be described as a function of the liquid phase fugacity coefficient $\hat{\phi}_i^{L}$.

Eq. 2.4 $$\hat{f}^{L} = x_i^{L} \hat{\phi}_i^{L} P$$

When both the vapour and the liquid phase fugacities are calculated from the fugacity coefficients (ϕ-ϕ approach), the basic VLE equation (Eq. 2.2) becomes:

Eq. 2.5 $$x_i^{V} \hat{\phi}_i^{V} = x_i^{L} \hat{\phi}_i^{L}$$

An alternative procedure results when the liquid phase fugacities are eliminated in favour of the activity coefficients, i.e. the ϕ-γ approach used in this work. The fugacity of component *i* in the liquid phase is expressed as a function of the activity coefficient $\hat{\gamma}_i^{L}$ and of the standard state fugacity $f_i^{L,\circ}$, chosen as the fugacity of the pure liquid *i* at the system temperature and pressure.

Eq. 2.6 $$\hat{f}_i^L = x_i^L \hat{\gamma}_i^L f_i^{L,\circ}$$

The standard state fugacity depends on the vapour pressure of pure component *i* at the system temperature (P_i^{Sat}), and on the saturated liquid fugacity coefficient of the pure component *i* ($\phi_i^{L,Sat}$) at the system temperature. The effect on the liquid fugacity of the difference between the system pressure and the vapour pressure is represented by the exponential term in Eq. 2.7, i.e. the Poynting pressure correction. The basic VLE equation given in Eq. 2.2 thus becomes:

Eq. 2.7 $$x_i^V \hat{\phi}_i^V P = x_i^L \hat{\gamma}_i^L P_i^{Sat} \phi_i^{L,Sat} \exp\left(\frac{1}{RT} \int_{P_i^{Sat}}^{P} V_i^L \right)$$

The Poynting correction is calculated from the molar volume of component *i* in the liquid phase. In this work, the molar volume was obtained from the Rackett equation of state (EOS) [59].

2.1.2 Gas- liquid equilibrium (GLE)

Gas-liquid equilibrium (GLE, also called gas solubility) is a particular case of vapour-liquid equilibrium, where at least one of the components is in supercritical state. Equivalently to the case of VLE, the ϕ-γ approach can be used for GLE [1].

The equilibrium equation for the subcritical component *i* is given by Eq. 2.7, when the standard state fugacity is chosen as the fugacity of the pure liquid *i* at the system temperature and pressure. The GLE equation for the supercritical compound *j* is

Eq. 2.8 $$x_j^V \hat{\phi}_j^V P = x_j^L \hat{\gamma}_j^* H_{j,S} \exp\left(\frac{1}{RT} \int_{P_j^{Sat}}^{P} V_j^L \right)$$

The activity coefficient of species *i* is normally defined according to the symmetric normalisation, i.e. $\hat{\gamma}_i = 1$ when $x_i^L = 1$ or, in other words, the activity coefficient of *i* approaches unity when *i* becomes pure. In this case the standard state fugacity may be regarded as the normalising factor, according to Eq. 2.6.

Eq. 2.9 $$\hat{f}_j^{L,id} = H_{j,S} x_j^L$$

Eq. 2.10 $$\hat{\gamma}_j^* = \frac{\hat{f}_j^L}{x_j^L H_{j,S}}$$

For a solute j, whose ideal behaviour is described based on Henry's law (Eq. 2.9), the activity coefficient $\hat{\gamma}_j^*$ is normalised using the Henry's law constant $H_{j,S}$, as shown in Eq. 2.10. In this case, the activity coefficient is called unsymmetric, and it approaches unity when species j becomes infinitely diluted, i.e. $\hat{\gamma}_j^* = 1$ when $x_j^L = 0$. Unsymmetrically and symmetrically normalised activity coefficients are completely interconvertible by means of the infinite dilution activity coefficient $\hat{\gamma}_i^\infty$.

Eq. 2.11 $$\hat{\gamma}_i^* = \frac{\hat{\gamma}_i}{\hat{\gamma}_i^\infty}$$

The unsymmetrically normalised activity coefficients are normally used for solutes, supercritical compounds, and ions in electrolyte systems.

The Henry's law constant is specific for a solute in a certain solvent (S). For single solvents, the Henry's law constant is a function of temperature. For multicomponent solvents, the Henry's law constant may depend not only on temperature, but also on the composition of the solvent.

2.1.3 Solid-liquid equilibrium (SLE)

In the case of SLE, Eq. 2.1 becomes:

Eq. 2.12 $$\hat{f}_i^S = \hat{f}_i^L$$

The liquid phase fugacity is described by Eq. 2.6. The solid phase fugacity is a function of the standard state fugacity $f_i^{S,\circ}$ and of the solid phase activity coefficient $\hat{\gamma}_i^S$.

Eq. 2.13 $$\hat{f}_i^S = x_i^S \hat{\gamma}_i^S f_i^{S,\circ}$$

Eq. 2.12 thus becomes:

Eq. 2.14 $$x_i^S \hat{\gamma}_i^S f_i^{S,\circ} = x_i^L \hat{\gamma}_i^L f_i^{L,\circ}$$

In this work, Eq. 2.14 was simplified into Eq. 2.17 according to [37, 60]. In most systems the pure solid crystallises out, thus the fugacity of the solid phase at equilibrium can be replaced by the fugacity of the pure solid, i.e. $x_i^S \hat{\gamma}_i^S = 1$ [60]. The ratio of the standard state fugacities can be evaluated from the conditions at the triple point by applying Eq. 2.15 to each phase. These considerations transform Eq. 2.14 into Eq. 2.16, when the volume difference ΔV is assumed independent of pressure.

Eq. 2.15 $$d\ln f = -\frac{\Delta H}{RT^2}dT + \frac{\Delta V}{RT}dP$$

Eq. 2.16 $$\ln\frac{f_i^{S,\circ}}{f_i^{L,\circ}} = \frac{\Delta H_{tp,i}}{R}\left(\frac{1}{T_{tp,i}} - \frac{1}{T}\right) - \frac{\Delta c_{p,i}}{R}\left(\ln\frac{T_{tp,i}}{T} - \frac{T_{tp,i}}{T} + 1\right) - \frac{\Delta V}{RT}\left(P - P_{tp,i}\right)$$

Eq. 2.16 is considerably simplified when the following assumptions apply:

1. The triple point temperatures are substituted with the melting point temperatures. Triple point temperatures are usually very nearly the same as atmospheric melting points, and the latter are more often known [37].
2. The pressure correction is considered negligible, which is usually the case [37].
3. The heat-capacity correction is dropped since it is small in the vicinity of the melting point [37, 60].

The activity coefficient of component *i* in liquid phase can therefore be directly calculated from melting point data as follows:

Eq. 2.17 $$\ln\left(x_i^L\hat{\gamma}_i^L\right) = -\frac{\Delta H_{fus,i}}{RT}\left(1 - \frac{T}{T_{fus,i}}\right)$$

2.2 Fugacity coefficients

The evaluation of the fugacity coefficient of component *i* in vapour phase requires the availability of a PVT EOS, i.e. an equation in the form $f(P,V,T)=0$ describing the volumetric behaviour of *i* as a function of pressure and temperature. In fact, the fugacity coefficient can be expressed according to Eq. 2.18 as a function of the compressibility factor Z.

Eq. 2.18 $$\ln \hat{\phi}_i^V = \int_0^P (\overline{Z}_i - 1)\frac{dP}{P}$$

In this work, the virial equation of state was used in [III]; otherwise the Soave-Redlich-Kwong (SRK) was the chosen EOS [II, IV, V]. The virial EOS [1] is either volume-explicit (the virial equation in pressure) or pressure-explicit (the virial equation in density). In this work, the density form of the virial equation was used.

The Soave-Redlich-Kwong (SRK) [37, 61] equation of state is the modification made by Soave of the Redlich-Kwong (RK) [62] EOS. Soave improved the performances of the RK EOS by developing the dependence on temperature of the attractive parameter a. Soave multiplied the RK $a(T,\omega)$ with a new temperature dependent parameter α_{SRK}. When the SRK EOS is applied to a mixture, mixing rules are used to calculate the EOS parameters. In this work, linear mixing rules were used for the co-volume parameters b (Eq. 2.19) and quadratic mixing rules for the attractive parameters a (Eq. 2.20 and Eq. 2.21). The binary interaction parameters k_{ij} were set to zero.

Eq. 2.19 $$\hat{b} = \sum_{i=1}^{N} x_i^V b_i$$

Eq. 2.20 $$\hat{a}\hat{\alpha}_{SRK} = \sum_{i=1}^{N}\sum_{j=1}^{N} x_i^V x_j^V (a\alpha_{SRK})_{ij}$$

Eq. 2.21 $$(a\alpha_{SRK})_{ij} = (1-k_{ij})\sqrt{(a\alpha_{SRK})_i (a\alpha_{SRK})_j}$$

2.3 Activity coefficients

Activity coefficients are determined principally from phase-equilibrium measurements, in particular from vapour-liquid and liquid-liquid equilibrium data [37]. Freezing point

depression data (SLE) are also used in special cases, such as the alkanolamine-water systems, in which one of the components has very low vapour pressure [35].

There are many equations correlating activity coefficients with composition mostly using mole fractions x_i, but occasionally also volume fractions Φ_i. Sometimes, activity coefficients are also expressed as a function of temperature.

In design of chemical units, semi-empirical models with a small amount of parameters are often preferred. Commonly used activity coefficients models are the Wilson [63], the NRTL [36] and the UNIQUAC [64]. The superiority of one method over the others is not always clear, and it often depends on the chemical system. Among these three semi-empirical models, the Wilson model better describes the greatest amount of chemical systems, while NRTL better describes aqueous systems [37].

If the experimental data for a specific system are scarce, the activity coefficients can be calculated by means of predictive methods. The UNIFAC [65] and UNIFAC-Dortmund [66] models are commonly used. They are based on the group contribution theory, which states that many properties of complex molecules can be approximated assuming that a smaller group of atoms within the molecule contributes to that property in a fixed way. The group contributions are optimised using a large amount of experimental data. The original UNIFAC and the UNIFAC-Dortmund differ in the values of the group contributions. The group contributions for the UNIFAC models used in this work were updated until the work by Wittig et al. [67], while in the case of the UNIFAC-Dortmund until Gmehling et al. [68].

Another predictive approach is that of COSMO-RS [69] and COSMO-SAC [70]. COSMO-RS treats the molecules as a unity, in opposition to the group contribution theory. The molecule surface is charged and the charge density is calculated via quantum mechanical calculations. The interactions between surfaces are statistically estimated. COSMO-SAC is a modification of COSMO-RS that predicts the intermolecular interactions based on the molecular structure with the help of a few adjustable parameters.

All of the above mentioned models were used at various extents, but the non-random two-liquid model (NRTL) [36] model was especially important in this work. In fact, NRTL is particularly suitable for describing aqueous systems [37], and it was

successfully applied by many research groups in modelling aqueous systems of alkanolamines [35, 45-48]. For these reasons, the NRTL model was used in this work to describe the activity coefficients of water +DIPA and water + MDEA.

2.3.1 The NRTL model

The NRTL model was chosen for aqueous binary systems, because of its simplicity and its wide use in design of chemical units. The equations of the NRTL model, as it was used in this work, are given in from Eq. 2.22 to Eq. 2.27. The adjustable binary model parameters are the symmetric non-randomness factor α_{ji}, and the asymmetric energy parameter τ_{ji}. The non-randomness parameter α_{ji} was treated as an empirical parameter, and it was given the value that best fitted the experimental data. This approach is in accordance with the work by Mato et al. [71] among others.

Eq. 2.22
$$\ln \hat{\gamma}_i = \frac{\sum_{j=1}^{m} \tau_{ji} G_{ji} x_j}{\sum_{l=1}^{m} G_{li} x_l} + \sum_{j=1}^{m} \frac{x_j G_{ji}}{\sum_{l=1}^{m} G_{lj} x_l} \left(\tau_{ij} - \frac{\sum_{n=1}^{m} x_n \tau_{nj} G_{nj}}{\sum_{l=1}^{m} G_{lj} x_l} \right)$$

Eq. 2.23 & 2.24
$$\tau_{ji} = \frac{\left(g_{ji} - g_{ii}\right)}{RT} \qquad G_{ji} = \exp\left(-\alpha_{ji} \tau_{ji}\right)$$

Eq. 2.25 & 2.26
$$\tau_{ii} = \tau_{jj} = 0 \qquad G_{ii} = G_{jj} = 1$$

Eq. 2.27
$$\tau_{ji} = \frac{b_{ji}}{T} + a_{ji}$$

In this work, only binary non-electrolyte systems were modelled. In the case of water + alkanolamine systems, these binary non-electrolyte systems are part of ternary electrolyte systems, such as CO_2 + water + alkanolamines. The work presented in this dissertation may be used in the future development of an electrolyte model for gas solubility. Several electrolyte models may be used for the solubility of CO_2 in aqueous alkanolamine solutions, such as the electrolyte-NRTL, the UNIQUAC electrolyte and their modifications [48, 72]. In particular, the electrolyte NRTL (e-NRTL) will allow the direct use of the NRTL parameters for the binary systems provided in this dissertation, thus showing the impact of this work on future research. For this reason, the e-NRTL model is here briefly introduced.

The e-NRTL [73-79]. has been extensively used for aqueous strong electrolytes and aqueous organic electrolytes, for weak electrolytes, strong acids and mixes solvent electrolytes. The e-NRTL was applied by many researchers to model the activity coefficients of sour gases + water + alkanolamines systems (e.g. [34, 45, 54, 80]). The original e-NRTL model is continuously revised and improved, when applied to sour gas systems [48]).

In the case of mixed-solvent solutions, the electrolyte NRTL model describes the excess Gibbs energy as the sum of three contributions. The short-range species interactions are described using the non-random two-liquid approach [73], the Pitzer-Debye-Hückel [81] formula is used to account for the long-range electrostatic interactions, and the Born equation [82] is utilized to model the Gibbs free energy of transfer of the ionic species from the infinite dilution state in a mixed solvent to the infinite dilution state in the aqueous phase [79]. The short-range interaction model assumes that there are three types of local composition interactions. The first type has a molecule as the central species interacting with other molecular species, cationic species or anionic species. The other two types of interactions have ether an anion or a cation as the central species. The surrounding species are either molecules or oppositely charged ions [76]. The models adjustable parameters are the same as in the NRTL model, i.e. the symmetric non-randomness factor α_{ji}, and the asymmetric energy parameter τ_{ji}. The species i and j derive from the model interactions leading to three types of binary parameters: molecule-molecule, molecule-electrolyte and electrolyte-electrolyte parameters [76].

The activity coefficients of the binary sub-system of water + alkanolamine have a strong influence on the predictions of the solubility of CO_2 or H_2S in alkanolamine solvents, especially at low gas absorption levels. While modelling the solubility of sour gases in alkanolamine solutions, the NRTL parameters of the binary system of water + alkanolamine can be used in the e-NRTL models to describe the interaction between the solvent molecules. In fact, the e-NRTL reduces to the standard NRTL model if applied to non-electrolytic systems.

3 Experimental procedures

In this work, several experimental methods were employed to measure phase equilibria of various systems. A static total pressure apparatus was used to measure the binary VLE of butane in alcohols (methanol, 2-propanol, 1-butanol, 2-butanol and 2-methyl-2-propanol) [V], and of diethyl sulphide in C_4 -hydrocarbons (1-butene, cis-2-butene, 2-methylpropane, 2-methylpropene, n-butane, trans-2-butene) [IV]. The same equipment was then modified to measure the VLE of water + DIPA and water + MDEA at high amine contents [II].

Another static total pressure apparatus, suitable for gas solubility measurements, was constructed, and the solubility of carbon dioxide in water + DIPA was measured. The same equipment also simultaneously measured the density of the carbonated aqueous solvent. The solubility of CO_2 in water + DIPA and water + MDEA was also measured at atmospheric pressure with a bubbling apparatus developed and constructed in this work. The solubility data obtained with the two techniques were compared against each other, and against literature data [III].

The SLE of water + DIPA and water + MDEA was measured with two experimental procedures, i.e. by means of a Differential Scanning Calorimeter (DSC), and with a method based on the visual observation of the melting point (visual method). The DSC was also used to measure the enthalpy of fusion of pure DIPA. The two experimental techniques for SLE measurements were validated against literature data, and their performances were compared with each other [II].

3.1 Vapour-Liquid Equilibrium measurements

3.1.1 Static total pressure apparatus for VLE measurements

The main feature of a static total pressure apparatus is that VLE data of binary systems are measured without the analysis of the equilibrium composition of the two phases. The equilibrium compositions of the liquid and vapour phase are calculated from the measured temperatures, pressures, and initial compositions, in addition to the dimensions of the equipment.

The experimental set-up and procedure used in this work were the same that were used by Uusi-Kyyny et al. [83]. A schematic representation of the equipment is given in [IV] and [V]. For the measurements of the systems of C_4 -hydrocarbons + diethyl sulphide the original equilibrium cell (AISI 316L) was substituted with a cell made of Hastelloy C-276 to avoid corrosion. The cell was sealed with a gold plated pressurised stainless steel o-ring.

For each binary system, the VLE curve was constructed by measuring the equilibrium points starting from both ends of the composition range. In practice, a pre-calculated amount of component 1 was injected to the equilibrium cell via a syringe pump. Subsequent additions of component 2 were made with a second syringe pump until the point of equimolarity was reached. The measurement then continued by repeating the same procedure starting from component 2 with subsequent additions of component 1. The coincidence of the two half-curves at equimolar composition was a clear indication of the success of the measurement.

A typical source of experimental error in measuring VLE data using a static total pressure apparatus is the presence of residual gases either in the equipment, or in the chemicals. Therefore, great care was taken in evacuating the equipment, and degassing the compounds before each measurement. The degassing equipment is schematically shown in Figure 3.1.

The equilibrium composition of the liquid and vapour phases were calculated from the total pressure data by means of the Barker method [83, 84]. More details on this experimental procedure are given in [IV] and [V].

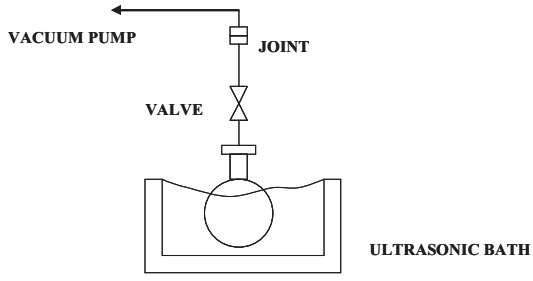

Figure 3.1 Degassing equipment.

3.1.2 Modifications of the static total pressure apparatus for VLE measurements of aqueous alkanolamine systems

The same static total pressure apparatus described in 3.1.1 was used to measure water + alkanolamine systems with some modifications in set-up and procedure. Total pressure VLE of water + alkanolamine systems is accurate only at high amine concentrations, due to the extremely low vapour pressure of alkanolamines [35]. For this reason, the measurements did not cover the whole composition range, but they were conducted only starting from pure alkanolamines and subsequently adding water. The pre-calculated amount of alkanolamine, i.e. DIPA or MDEA, was manually fed to the equilibrium cell with a syringe, which was accurately weighted before and after injection. The use of a syringe pump was discouraged by the high viscosity of the amines. DIPA is a solid at room temperature; therefore it was heated above its melting point, i.e. $T_{fus} = 315.8K$, prior to feeding. The amines were degassed when in the equilibrium cell. Subsequent injections of water were performed with a syringe pump, and the VLE curve was constructed. Details on this experimental procedure are given in [II].

3.2 Gas Liquid Equilibrium (GLE) measurements

3.2.1 Static total pressure apparatus for GLE measurements

The solubility of CO_2 in water + DIPA was measured with the equipment shown in Figure 3.2, which was constructed and developed in this work. As this equipment is also a static total pressure apparatus, the composition of the liquid phases was not analysed, but it was calculated from the injected material, the size of the equipment, and the measured temperatures, pressures and densities.

The solubility measurements were conducted by injecting a known amount of solvent to the equilibrium cell with a syringe pump. Solvent degassing and apparatus evacuation are fundamental steps in gas solubility measurements. The solvent was degassed in an ultrasonic bath with a procedure similar to the one used for VLE measurements (Figure 3.1). Since the solvent was a solution, its composition varied during degassing, mainly due to the evaporation of water. The solvent composition was analysed by refractometry using a sample of the residual degassed solution. Once the desired amount of solvent was

in the cell, CO_2 was added and the equilibrium point was measured, i.e. the equilibrium temperature and pressure in the cell were measured. The amount of injected gas was calculated from the pressure in the CO_2 feed cylinder, which was measured before and after the gas injection. The system was considered at equilibrium when the pressure in the cell was constant for at least 1.5 h. Even under vigorous stirring, the system took about 4 h to reach equilibrium. The solubility curves were constructed at constant temperature by subsequent gas additions. The experimental run was concluded at a total pressure of ca. 1 MPa, in order to comply with the range of the pressure transducer situated in the equilibrium cell. More details on the experimental procedure and on the instrumentation are given in [III].

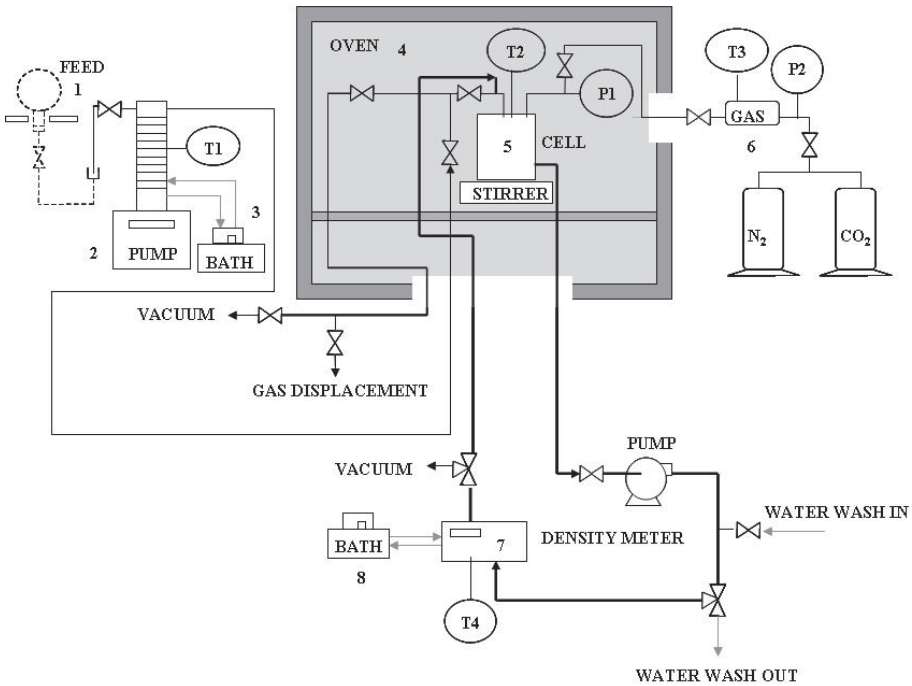

Figure 3.2 Static total pressure apparatus: (1) 250 cm^3 round bottom flask for amine solution feed to the syringe pump; (2) 260 cm^3 syringe pump; (3) circular bath controlling the temperature of the syringe pump; (4) oven (bottom hole Ø= 10 cm, side hole Ø= 2.5 cm); (5) equilibrium cell; (6) CO_2 feed cylinder; (7) density meter; (8) circular bath controlling the temperature of the density meter; ▬ recirculation lines; — water lines; T1, T2, T3 and T4 temperature probes, P1 and P2 pressure transducers.

As it is customary in alkanolamine systems (e.g. [25, 26, 40]), the solubility of CO_2 in the aqueous solvents was expressed as loading (α):

Eq. 3.1 α = moles of absorbed CO_2 / moles of amine

In calculating this quantity from the measured variables, it was assumed that the amount of moles of alkanolamine in the liquid phase was constant during the experimental run, and it was equal to the amount of moles of amine in the degassed solvent. This assumption is justified by the low vapour pressure of alkanolamines [23, 85]. The virial equation of state [1] in density truncated to the third virial coefficient was used to calculate the moles of CO_2, as it is described in [III]. The mole fraction of CO_2 in the liquid phase was also estimated for comparison purposes.

The experimental method was validated by measuring the solubility of CO_2 in water at 298.57 K. Our results were compared with literature data [86-92] in terms of Henry's law constant of CO_2 in water ($H_{1,W}$), and of mole fraction of CO_2 in the liquid phase (x_1^L). These quantities were calculated from the measured variables according to the ϕ-γ model for the reduction and correlation of solubility data by Van Ness and Abbott [1] for single solute / single solvent systems. In the approach by van Ness and Abbott [1], some assumptions are suggested in order to simplify the basic GLE equation, i.e. Eq. 2.8, thus facilitating the data reduction procedure. The Poynting correction and the activity coefficient of the solvent were assumed equal to unity. The molar volume V_1^L of the solute was assumed constant, and equal to the infinite dilution molar volume $V_1^{L,\infty}$, according to the Krichevsky-Kasarnovsky [93] correction. Eq. 2.8 thus becomes

Eq. 3.2 $$x_1^V P\hat{\phi}_1^V = x_1^L \gamma_1^* H_{1,W} \exp\frac{V_1^{L,\infty}\left(P - P_1^{sat}\right)}{RT}$$

The unsymmetric activity coefficient of the solute was modelled according to Eq. 3.3, as suggested by van Ness and Abbott [1].

Eq. 3.3 $$\ln\left(\gamma_1^*\right) = A\left(\left(x_2^L\right)^2 - 1\right)$$

The Henry's law constant of CO_2 in water measured in this work was 5.9 MPa smaller than that of Fonseca et al. [86], while it agreed with all the other sources [87-91] within the experimental uncertainty. In terms of mole fraction, the maximum deviation between

our work and the data found in the literature [91, 92] was of 0.00012 with the work by Carroll et al. [91]. The results of the validation are reported in [III].

3.2.2 Bubbling apparatus

The solubility of CO_2 in aqueous solutions of water + DIPA and water + MDEA at atmospheric pressure was measured at various temperatures and solvent compositions with a bubbling apparatus. The apparatus and the associated analytic technique were developed is this work, based on the volumetric calcimeter suggested by Loeppert and Suarez [94], and on the bubbling cell described by Hovorka and Dohnal [95].

A schematic representation of the equipment is given in Figure 3.3. The bubbling cell was composed of a presaturator and the equilibrium cell, also indicated as dilution cell. The function of the presaturator, which was filled with distilled water, was to wet the gas in order to keep constant the amount of solvent in the dilution cell. The measurements with the bubbling apparatus were isobaric. An alkanolamine solution of known composition was filled into the dilution cell, and the temperature was stabilised to the desired value by means of a water bath that circulated water through the jacket of the bubbling cell. CO_2 was bubbled through the alkanolamine solution via the presaturator until the solution reached saturation. It was found with preliminary tests that the time to reach equilibrium with the bubbling equipment depended on the temperature and on the composition of the solvent, and it could be up to 2 weeks. At saturation, the temperature and pressure were recorded, and 3-4 samples of the saturated solution were taken for analysis with the volumetric calcimeter (Figure 3.4). Another equilibrium point was then measured by changing the temperature.

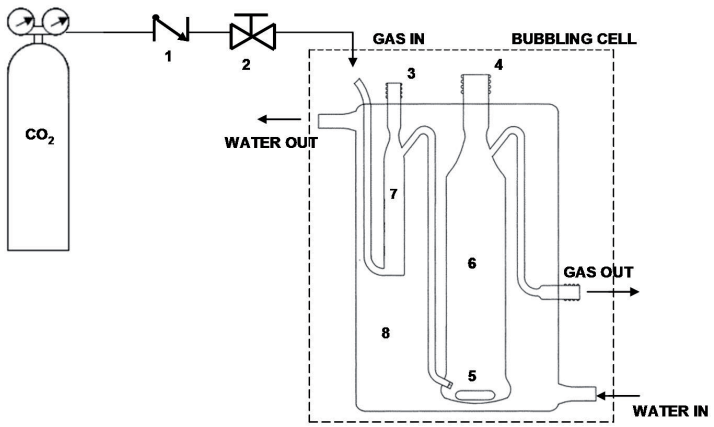

Figure 3.3 Bubbling equipment with Hovorka-type bubbling cell [95]. (1) Check valve; (2) needle valve; (3) filling opening to the presaturator; (4) filling and sampling opening to the cell; (5) magnetic stirrer; (6) dilution cell; (7) presaturator; (8) thermostated jacked. Water was used as thermostatic liquid.

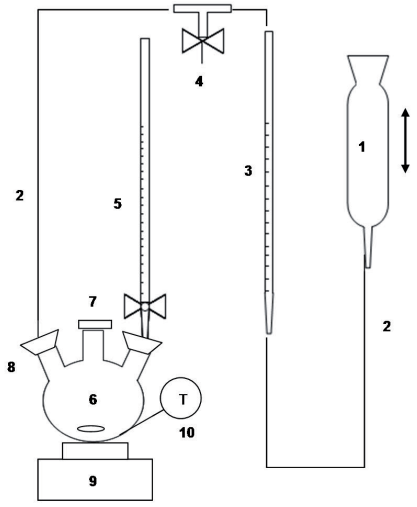

Figure 3.4 Volumetric calcimeter [94]. (1) Leveling bulb; (2) flexible tubing; (3) manometer (50 ml); (4) pressure release valve; (5) HCl burette with stopcock (25 ml); (6) three-neck round-bottom flask (250 ml); (7) ground glass taper joint stopper; (8) ground glass joint connected to the manometer; (9) magnetic stirrer; (10) temperature probe.

The volumetric calcimeter was used to measure the moles of CO_2 in the liquid phase using the procedure described in [94]. An excess amount of aqueous HCl was used to release the absorbed CO_2 from the sampled solution in the round bottom flask. The released gas pushed the liquid contained in the manometer permitting the determination

of the gas volume. The conversion between the volume of released gas and the moles of CO_2 was made based on a calibration of the apparatus obtained by analysing known amounts of Na_2CO_3 in water.

The mole fraction of CO_2 in the liquid phase was calculated from the absorbed moles of CO_2, from the initial composition of the alkanolamine solution, and from the weight of the sample. As mentioned above, for each equilibrium point 3-4 samples of the saturated solution were taken. Each sample was analysed, i.e. 3-4 analysis of the same equilibrium composition were performed for each equilibrium point. The mole fraction of CO_2 in the liquid phase was the average of the mole fractions of CO_2 resulting from the analysis of all the samples. Details about this experimental technique and the instrumentation used are given in [III].

The bubbling system of CO_2 + water + MDEA was used to validate the experimental technique by means of a comparison with solubility values found in the literature [27-34].

3.3 Solid-Liquid Equilibrium measurements

The SLE of binary systems of water + alkanolamines was measured by means of two experimental techniques (the visual method and a Differential Scanning Calorimeter), and the results were compared with each other. The purpose of this comparison was not only to validate the experimental results, but also to compare the performances of the relatively inexpensive visual method with an advanced technique such as DSC. SLE data are more appropriate than VLE data to obtain the activity coefficients of water + alkanolamine systems at low amine concentrations. This is due to the low vapour pressure of alkanolamines [35]. Details on the two experimental techniques are given in [II].

3.3.1 Visual method

The melting point of water + MDEA and water + DIPA solutions was measured at atmospheric pressure in the apparatus shown in Figure 3.5. A similar equipment was used by Jakob et al. [60]. A sample of a gravimetrically constructed solution of water + alkanolamine was injected in the equilibrium cell. The solution was supercooled with

liquid nitrogen, and the cell was then installed in the thermostated jacket. Glycol was used instead of water in the thermostating bath since the equilibrium temperatures were below the freezing point of water. The solution was slowly heated, and the melting process was observed visually. The temperatures in the cell and in the jacket were recorded as a function of time throughout the whole experimental run. This information was used to support the visual observation of the melting point. Each melting point was measured at least twice, and the average value of these measurements was given as the experimental result.

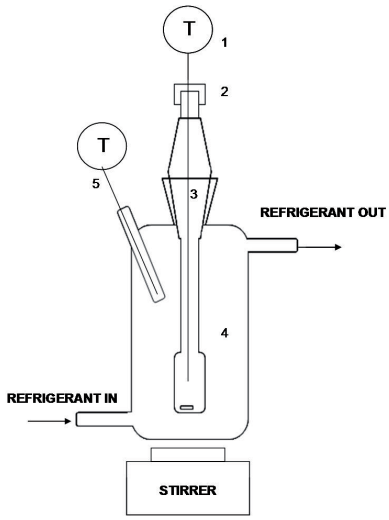

Figure 3.5 Apparatus for the visual measurement of SLE. (1) and (5) temperature probes; (2) screw cap with septum (3) equilibrium cell (4) thermostated jacket. A thermostated bath circulated the refrigerant through the jacket.

3.3.2 Differential Scanning Calorimeter (DSC)

The melting point of the systems of water + MDEA and water + DIPA was measured with a Perkin-Elmer Diamond Differential Scanning Calorimeter equipped with liquid nitrogen cooling system. The alkanolamine solutions were prepared gravimetrically. Samples of these solutions were accurately weighted, and sealed in aluminium pans. The cooling and heating of the samples during the measurements was performed at a constant rate of 10 ºC/min, and an empty crucible was used as reference. The DSC was calibrated with high-purity indium with a heating rate of 10 ºC/min.

3.4 Estimation of the experimental uncertainty

No measurement, however carefully made, can be completely free of uncertainties. In this work, great importance was given to the estimation of uncertainties, not only for measured quantities, but also for the calculated variables that were derived from the measured quantities.

When possible, the uncertainty of a measured variable was identified with the uncertainty of the instrument that measured it. Not only the instrument resolution and accuracy, but also its calibration contributed to the uncertainty of the instrument. This definition of uncertainty applied to all the temperatures, pressures, densities and volumes measured during VLE and GLE experiments. In some cases, a quantity is not directly measured with an instrument, but it results from the interpretation of the response of an analytical technique. This was the case of the mole fractions analysed with the volumetric calcimeter, and of the melting points measured with the DSC and the visual method. The uncertainty of these variables was estimated based on considerations that were specific to the analytical technique.

Due to the characteristics of the experimental methods, the composition of the vapour and of the liquid phase in VLE measurements, and the gas solubility in GLE measurements were calculated quantities. In [V] the uncertainty δq of a derived variable $q = q(s,....,u)$ was estimated by calculating q' when all the measured variables $(s,....,u)$ assumed their minimum $(s^- = s - \delta s,....,u^- = u - \delta u)$ or their maximum values $(s^+ = s + \delta s,....,u^+ = u + \delta u)$. The uncertainty of the calculated variable was the maximum deviation between q and q' according to Eq. 3.4.

Eq. 3.4 $$\delta q = \max\left| q - q'\left(s^-,....,u^-\right); q - q'\left(s^+,....,u^+\right)\right|$$

This method gives an estimate of δq, but it does not necessarily calculate the absolute maximum uncertainty. The absolute maximum uncertainty was obtained when the matrix of all the possible combinations of the values assumed by the measured variables was constructed, i.e. δq was calculated according to Eq. 3.5.

Eq. 3.5 $$\delta q = \max\left|q - q'\left(s^-,....,u^-\right); q - q'\left(s^+,....,u^+\right); q - q'\left(s^+,....,u^-\right); q - q'\left(s^-,....,u^+\right);...\right|$$

δq was estimated with Eq. 3.5 in [IV]. The likelihood of the absolute maximum uncertainty actually occurring during the experimental work is rather small; therefore this approach usually overestimates the uncertainty of the derived variables.

In [III] and [II] the uncertainty of the calculated variables was estimated according to the error propagation theory developed by Taylor [96]. The error propagation theory states that δq is given by Eq. 3.6 if the measured quantities are independent and random, otherwise it is estimated by Eq. 3.7.

Eq. 3.6 $$\delta q = \sqrt{\left(\frac{\partial q}{\partial s}\delta s\right)^2 + \ldots + \left(\frac{\partial q}{\partial u}\delta u\right)^2}$$

Eq. 3.7 $$\delta q \le \left|\frac{\partial q}{\partial s}\right| \cdot \delta s + \ldots + \left|\frac{\partial q}{\partial u}\right| \cdot \delta u$$

A summary of the uncertainty analysis for each variable as it was estimated in this work is given in Table 3.1.

Table 3.1 Uncertainty analysis: overview by variable.

Variable	***Description***	***Type***	***Uncertainty***	***Ref.***
n_i	Initial moles of component i	Calculated	Error propagation theory	[V], [IV]
z_i	Initial mole fraction of i	Calculated	Error propagation theory	[V], [IV], [II]
T	Equilibrium temperature	Measured	Instrument	[V], [IV]; [III]; [II]
T (visual method and DSC)	Melting point	Measured	Considerations on analytics	[II]
P_{exp} or P	Equilibrium pressure	Measured	Instrument	[V], [IV], [III], [II]
P_{leg}	Calculated equilibrium pressure	Calculated	Eq. 3.4	[V]
P_{leg}	Calculated equilibrium pressure	Calculated	Eq. 3.5	[IV]
x_i	Equilibrium liquid mole fraction of i	Calculated	Eq. 3.4	[V]
x_i	Equilibrium liquid mole fraction of i	Calculated	Eq. 3.5	[IV]

Variable	*Description*	*Type*	*Uncertainty*	*Ref.*
x_i (static GLE apparatus)	Equilibrium liquid mole fraction of i	Calculated	Error propagation theory	[III]
x_i (bubbling apparatus)	Equilibrium liquid mole fraction of i	Measured	Considerations on analytics	[III]
x_i (static VLE apparatus and SLE)	Equilibrium liquid mole fraction of i	Calculated	Error propagation theory	[II]
y_i	Equilibrium vapour mole fraction of i	Calculated	Eq. 3.4	[V]
y_i	Equilibrium vapour mole fraction of i	Calculated	Eq. 3.5	[IV]
γ_i	Activity coefficient of i	Calculated	Eq. 3.4	[V]
γ_i	Activity coefficient of i	Calculated	Eq. 3.5	[IV]
$H_{i,j}$	Henry's law constant of i in j	Calculated	Error propagation theory	[III]
w_i	Weight fraction of i	Measured	Considerations on analytics	[III]
α	Loading	Calculated	Error propagation theory	[III]
T_d	Temperature in the density meter	Measured	Instrument	[III]
ρ	Density	Measured	Instrument	[III]
ΔH_{fus}	Enthalpy of fusion	Measured	Considerations on analytics	[II]

4 Results

A summary of all the experimental data points measured in this work is given in Table 4.1.

Table 4.1 Summary of all the experimental data measured in this work.

Equipment	*Data type*	*System type*	*System*	*T (K)*	*P (kPa)*	*Solvent (wt%)*	*N. points*	*Ref.*
Static total pressure (VLE)	VLE	Binary	Butane + methanol	364.5	298 - 1285		27	[V]
			butane + 2-propanol	364.5	144 - 1284		27	[V]
			butane + 1-butanol	364.5	37 - 1285		27	[V]
			butane + 2-butanol	364.5	74 - 1284		27	[V]
			butane + 2-methyl-2-propanol	364.5	143 - 1284		27	[V]
			DES + 1-butene	312.6	15 - 451		26	[IV]
			DES + cis-2-butene	312.6	15 - 333		26	[IV]
			DES + 2-methylpropane	308	13 - 460		25	[IV]
			DES + 2-methylpropene	312.6	15 - 466		26	[IV]
			DES + n-butane	317.6	19 - 427		26	[IV]
Static total pressure (VLE) Amine modification	VLE	Binary	water + MDEA	334 - 358	0 - 58		31	[II]
			water + DIPA	335 - 357	0 - 53		49	[II]
Static total pressure (GLE)	GLE Density	Binary	CO_2 + water	298.6	3 - 747		8	[III]
		Ternary	CO_2 + water + DIPA	298 - 303	2 - 956	10 - 34 $wt\%_{DIPA}$	36	[III]
Bubbling apparatus	GLE	Ternary	CO_2 + water + MDEA	298 - 333	94 - 103	10 - 49 $wt\%_{MDEA}$	14	[III]
			CO_2 + water + DIPA	298 - 353	87 - 103	10 - 35 $wt\%_{DIPA}$	28	[III]
Visual method	SLE	Binary	water + MDEA	259 - 273	atm.		7	[II]
			water + DIPA	259 - 273	atm.		9	[II]

Equipment	*Data type*	*System type*	*System*	*T (K)*	*P (kPa)*	*Solvent (wt%)*	*N. points*	*Ref.*
		Pure comp.	water		atm.		2	[II]
		Pure comp.	DIPA		atm.		1	[II]
DSC	SLE	Binary	water + MDEA	247 - 270	atm.		9	[II]
			water + DIPA	258 - 273	atm.		8	[II]
		Pure comp.	MDEA		atm.		1	[II]
			DIPA		atm.		1	[II]
	Enthalpy fusion	Pure comp.	DIPA		atm.		1	[II]

4.1 The miniplant concept applied to distillation design

The miniplant methodology was applied to the NExOCTANE process (Figure 1.1) for producing isooctane [2]. The validity of the thermodynamic vapour-liquid equilibrium model in a distillation column was tested with a miniplant column. The set up of the distillation column is given in [VI].

The most important binaries for VLE modelling the NExOCTANE process were identified as 2-methyl-2-propanol + alkanes, 2-methyl-2-propanol + alkenes and 2-methyl-2-propanol + water. In fact, the composition of the recycle stream containing the inhibitor 2-methyl-2-propanol must be accurately predicted to avoid unrealistic accumulation of this compound in the column during simulation. VLE data for the thermodynamic model of these systems were taken either from the literature [97-100] or they were measured in our research group [11, 101-106]. In particular, the VLE of the system of 2-methyl-2-propanol + butane was studied at 364 K in [V] as shown in chapter 4.2.

No adequate correlations for calculating the mass transfer coefficients and areas were found for the packing used in the miniplant column. Thus, a serie of test runs were performed to estimate the HETP (height equivalent to a theoretical plate) of the packing. The column was operated in total reflux to separate n-hexane and cyclohexane. It was found that the best way to simulate total reflux operation with our distillation model was by introducing a large feed into the reboiler, and forcing almost all the material to exit the

column as bottom product. The simulated compositions were matched with the measured compositions. Heat losses were important for simulating this small column. Thus, they were estimated for the condenser, for the reboiler and for the column body. The HETP was obtained by trial-and-error altering the number of theoretical stages to mach the experimental compositions [VI].

Test runs for the actual feed to the distillation column of the NExOCTANE process were performed. Thus, the VLE model of 2-methyl-2-propanol in hydrocarbons could be tested against miniplant data. The calculated HETP values were used in the column simulations, and both feed and stream locations were placed in accordance with the HETP calculations. Focus was placed on the composition of the key components in the product streams, i.e. isobutene, diisobutene and 2-methyl-2-propanol. The 2-methyl-2-propanol content was well predicted both in the top product and in the side draw. Globally, the VLE and the HETP models complemented each other to successfully represent the behaviour of the column [VI].

4.2 VLE of butane + alcohols

VLE data for the systems of butane + alcohols are presented in [V]. The measured vapour pressure of the pure components agreed with literature correlations [107-109]. The system of butane + methanol was of particular interest among the systems studied. The data points measured in this work at 364.5 K were compared with data found in the literature [6, 8] at temperatures close to 364 K in Figure 4.1. The bubble point measurements by Petty and Smith [6] showed a considerable disparity with other reported measurement, as it was also observed by Courtial et al. [4]. Their dew point measurements agreed with our measured data.

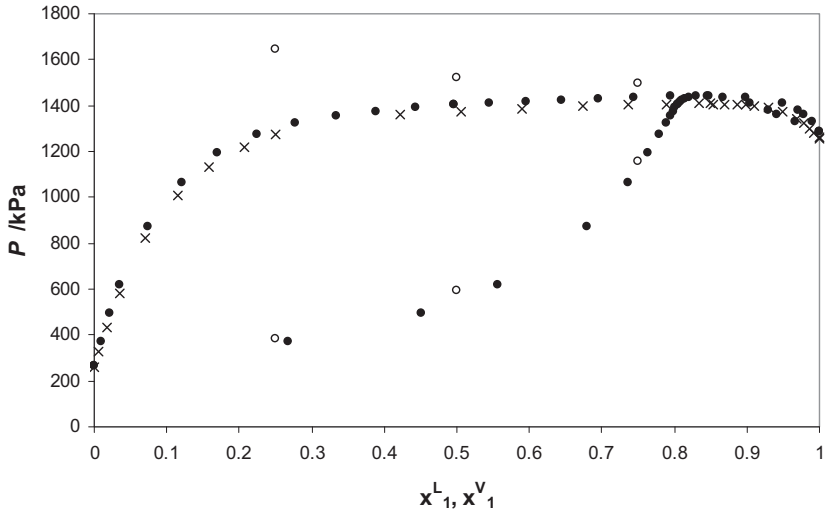

Figure 4.1 Pressure – composition diagram of butane (1) + methanol (2). (•) This work at 364.5 K; (×) Fischer et al. [8] at 363.31 K; (○) Petty and Smith at 366.45 K [6].

The system of butane + methanol evidenced azeotropic behaviour at 364.5 K. Several investigators proved the existence of an azeotropic point for this system at various temperatures [4, 7-11]. The azeotrope composition from this work is plotted in Figure 4.2 alongside literature data, and with the model for the temperature dependence of the azeotrope composition proposed by Leu et al. [9]. Our azeotrope composition and that of Moilanen et al. [11] agreed well with the model by Leu et al. [9] ($\left|\Delta x_1^L\right| < 0.0001$ in our work and $\left|\Delta x_1^L\right| < 0.003$ for Moilanen et al. [11]). Fischer et. al. [8] and Churkin et al. [7] observed a higher composition ($\left|\Delta x_1^L\right| = 0.01$ for Fischer et. al. [8] and $\left|\Delta x_1^L\right| = 0.03$ for Churkin et al. [7]. Leu et al. [9] also proposed a model for the dependency of the azeotrope pressure on temperature. The model is shown in Figure 4.3 alongside the experimental data. In the case of pressure, only the data point by Churkin et al. [7] deviated considerably from the model predictions ($\left|\Delta P\right| = 295$ KPa).

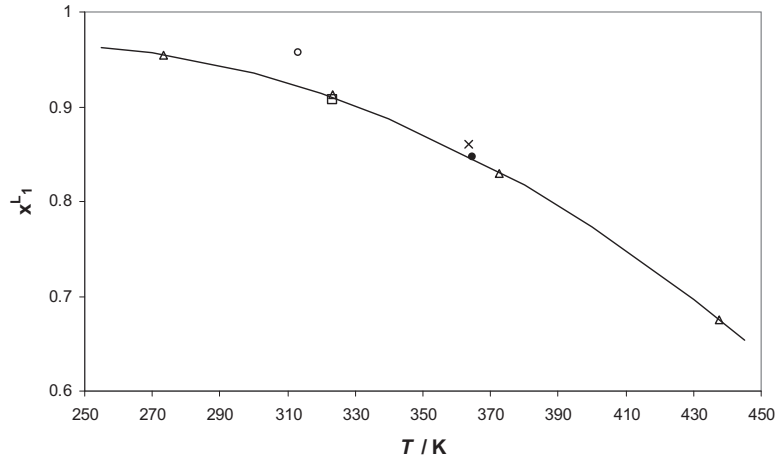

Figure 4.2 The azeotrope composition for the system of butane (1) + methanol (2) as a function of temperature. (•) This work; (×) Fischer et al. [8]; (Δ) Leu et al. [9,10]; (○) Churkin et al. [7]; (□) Moilanen et al. [11]; (—)Leu et al. [9] model.

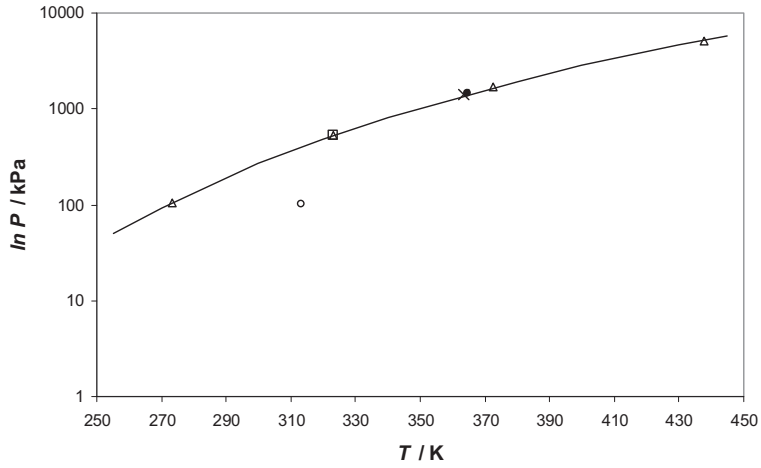

Figure 4.3 The azeotrope pressure for the system of butane (1) + methanol (2) as a function of temperature. (•) This work; (×) Fischer et al. [8]; (Δ) Leu et al. [9,10]; (○) Churkin et al. [7]; (□) Moilanen et al. [11]; (—)Leu et al. [9] model.

The system of butane + 1-propanol was measured at 363 K by Deak et al. [12]. A comparison with the data measured in this work is given in Figure 4.4. The system of butane + 2-methyl-2-propanol was of importance for the production of isooctane, as

presented in [VI]. The VLE of this system was measured at 364 K in this work [V] and at 323 K by our research group [11]. Melpolder [14] also measured butane + 2-methyl-2-propanol at 333 K, 358 K, 383 K and 408 K. A comparison of all these data is shown in Figure 4.5.

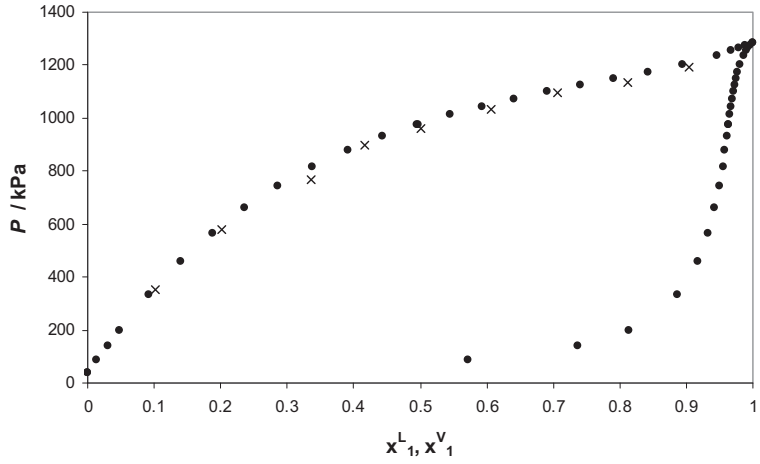

Figure 4.4 Pressure – composition diagram of butane (1) + 1-propanol (2). (•) This work at 364.5 K; (×) Deak et al. [12] at 363 K.

The activity coefficients of all the measured binary systems were modelled with the Wilson and the NRTL models. Both models gave comparable results in terms of pressure residuals. The highest residuals were obtained for butane + methanol. The activity coefficients were also predicted with the UNIFAC, UNIFAC Dortmund and the COSMO-RS models. The results of the model predictions and the model parameters are given in [V]. In general, among the predictive methods, COSMO-RS gave the best performances for butane + alcohols systems in terms of average absolute pressure residuals. In particular, COSMO-RS was the only predictive method that could describe satisfactorily the system of butane + methanol. UNIFAC-Dortmund either gave comparable or better prediction than the original UNIFAC.

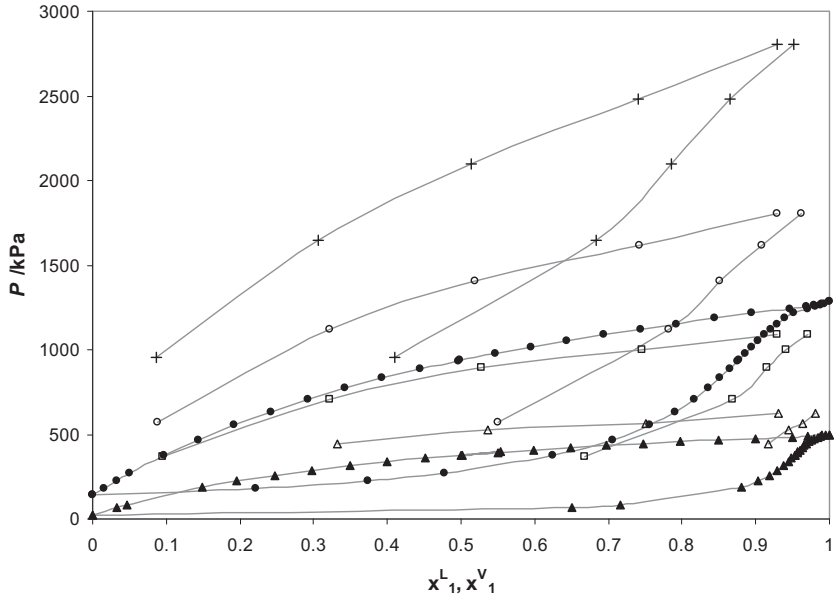

Figure 4.5 Pressure – composition diagram of butane (1) + 2-methyl-2-propanol (2). (•) This work at 364.5 K; (▲) Moilanen et al. [11] at 323.15 K; (+) Melpolder [14] at 408.15 K; (○) Melpolder [14] at 383.15 K; (□) Melpolder [14] at 358.15 K; (Δ) Melpolder [14] at 333.15 K.

In terms of activity coefficients (Figure 4.6 for the system of butane + methanol) the UNIFAC-Dortmund predicted best with respect to the activity coefficients calculated from our experimental data with the Legendre polynomial. COSMO-RS had a tendency to overestimate the infinite dilution activity coefficients of the alcohols. The infinite dilution activity coefficients reported by Fischer et al. at 363.39K for butane + methanol are included in Figure 4.6 with the results obtained in this work at 364.5 K.

All the predictive method recognised the azeotropic point of the system of butane + methanol. Our experimental data suggested that also the system of butane + 2-propanol may have an azeotropic point. UNIFAC and UNIFAC-Dortmund predicted an azeotropic point for butane + 2-propanol. COSMO-RS did not predict an azeotropic point for butane + 2-propanol, but for the system of butane + 2-methyl-2-propanol, which was not observed experimentally.

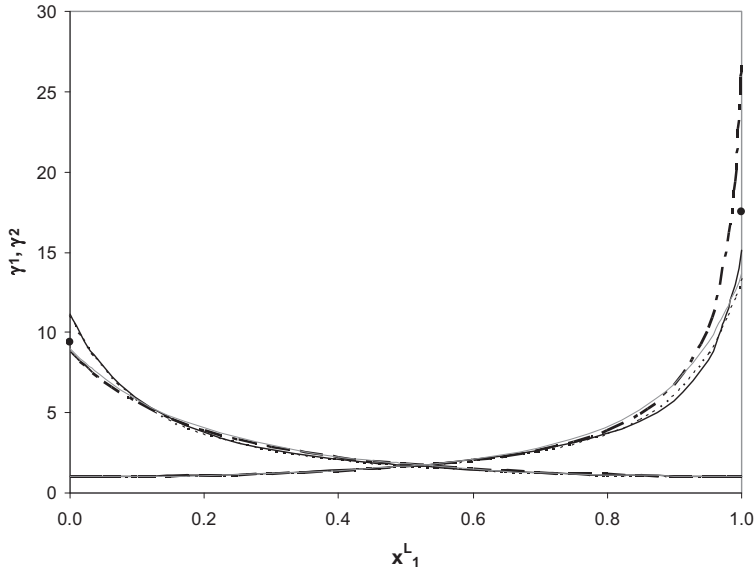

Figure 4.6 Activity coefficients of butane (1) + methanol (2). (—) This work, Legendre polynomial (364.5 K); (--) NRTL (364.5 K); (▬) UNIFAC-Dortmund (364.5 K); (□ -) COSMO-RS (364.5 K); (•) Fischer et al. [8](363.39 K).

4.3 VLE of diethyl sulphide + C_4 - hydrocarbons

VLE data for the systems of diethyl sulphide (DES) + C_4 hydrocarbons are presented in [IV]. The measured vapour pressure of the pure components agreed with literature correlations [107-109]. No data were found in the literature for comparison with the data measured in this work. The activity coefficients were modelled with the Wilson, NRTL and UNIQUAC models. They gave comparable results for all the systems modelled. The results of the fitting and the model parameters are given in [IV]. The VLE of the measured systems was predicted with the UNIFAC model, when the group contribution parameters were publicly available (2-methylpropane + DES and n-butane + DES). The measured VLE of the system of 2-methylpropane + DES is compared with the UNIFAC predictions in Figure 4.7. UNIFAC predicted almost ideal behaviour for both systems. The activity coefficients of all the systems were predicted with COSMO-SAC. COSMO-SAC overestimated the activity coefficients of all the components in the whole

composition range, compared to the activity coefficients calculated from our experimental data. In general, COSMO-SAC predicted better the systems of diethyl sulphide with C_4 -olefins than with C_4 -paraffines.

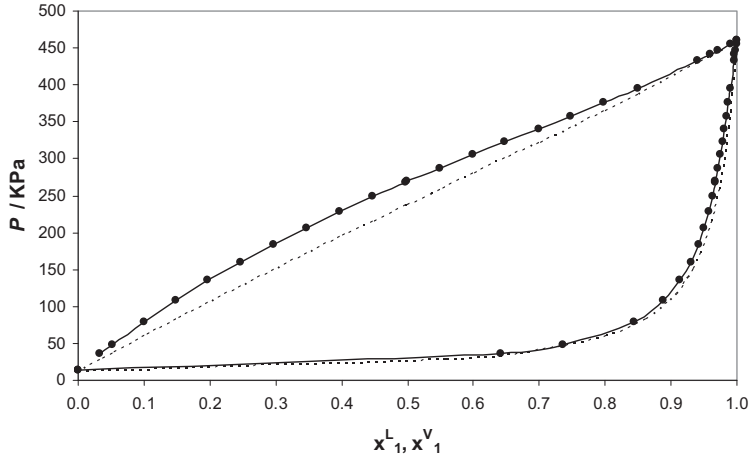

Figure 4.7 Pressure – composition diagram of 2 – methylpropane (1) + diethyl sulphide (2) at 308 K. (●) This work, (□) Wilson model; (- -) UNIFAC model.

4.4 Aqueous alkanolamine systems

Alkanolamine solvents are of great industrial importance both for refining and for carbon capture applications. Therefore, it was an important part of this work to supply experimental data with the scope of improving the thermodynamic model of these systems.

The main aspects involved in modelling the solubility of CO_2 in aqueous alkanolamine solutions are schematically shown in Figure 4.8. The systems of CO_2 + water + alkanolamine are highly reactive; therefore not only physical solubility and activity coefficient models, but also chemical reactions should be considered while dealing with these systems. In this work, a full model for the solubility of CO_2 in aqueous alkanolamine solutions is not developed. Experimental data and models of the non-reactive binary subsystems are studied. The grey boxes in Figure 4.8 represent the areas that were investigated in this dissertation, thus showing the impact of this work on future modelling of the solubility of CO_2 in aqueous alkanolamine solutions.

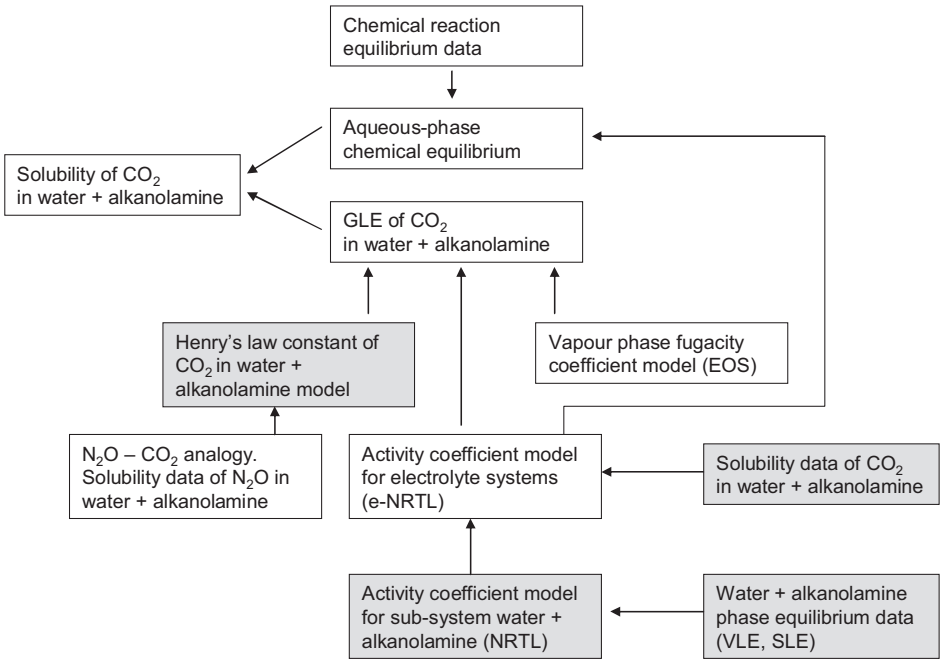

Figure 4.8 Modelling of the solubility of CO_2 in aqueous alkanolamine solutions. In grey are evidenced the areas studied in this work.

The description of the activity coefficients relies on solubility data, and on the accurate thermodynamic description of the mixed solvent. The activity coefficients of the solvent species are obtained from phase equilibrium data of the solvent. In the specific case of DIPA, scarcity of solubility data and absence of solvent phase equilibrium data limited the development of a model for aqueous DIPA systems. In fact, no satisfactory thermodynamic model for aqueous DIPA solvents was available in the open literature before this work. Therefore, new phase equilibrium data were considered of great importance for model development.

In addition, it was also noticed that many of the existing models for the Henry's law constant of CO_2 in alkanolamine solutions deviated highly from the experimental data at high temperatures, i.e. close to operative conditions in the alkanolamine solvent regeneration column. Thus, a new model for the Henry's law constant of CO_2 in alkanolamine solutions was developed, in which the Henry's law constant depended on

the temperature, and on the composition of the solvent. Particular attention was given to the model performances at high temperatures.

4.4.1 Solubility data of CO_2 in water + alkanolamine solvents

A summary of all the measured solubility data of CO_2 in water + MDEA and water + DIPA with the two equipments (GLE static and bubbling apparatus) is given in Table 4.1, and the data are presented in [III].

The solubility of CO_2 in water + DIPA measured in this work with the GLE static apparatus is plotted in Figure 4.9. A numerical comparison with literature data was not possible since no data at the same experimental conditions were found. Some of the data points by Isaacs et al. [25] and ter Maat [26] were included in Figure 4.9 for visual comparison. With respect to amine concentrations, the data in Figure 4.9 behave consistently, i.e. at the same temperature and partial pressure of CO_2, the loading is higher the lower is the amine concentration. Similarly, with respect to temperature, at the same amine concentration and pressure the loading is higher the lower is the temperature.

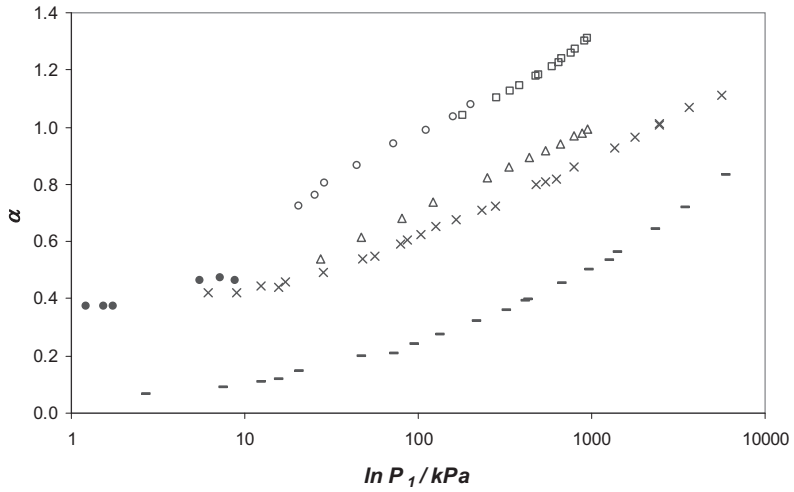

Figure 4.9 . Loading α = *[mole CO_2/ mole amine]* of CO_2 (1) in solutions of water (2) and DIPA (3) as a function of the partial pressure P_1 of CO_2. (○) This work, GLE static apparatus, w_3 = 10.1 % at 299.72 K ; (□) this work, GLE static apparatus, w_3 = 11.0 % at 298.22 K; (Δ) this work, GLE static apparatus, w_3 = 33.9 % at 298.29 K; (×) Isaacs et al. $w_3 \approx 33$ % at 313.15 K; (−) Isaacs et al. $w_3 \approx 33$ % at 373.15 K; (●) ter Maat et al. w_3 = 35 % at 298.15 K.

The density of carbonated aqueous solutions of DIPA was measured in the GLE static apparatus alongside the solubility. No density data of carbonate aqueous solutions of DIPA were found in the literature. The density of non-carbonated aqueous DIPA was measured by Henni et al. [110]. The density of non-carbonated aqueous DIPA measured in this work deviated from the work by Henni et al. [110] less then 0.2 %. The density data of carbonated solutions were correlated with the model by Weiland et al. [111]. The model details are reported in [III] alongside the measured densities. The deviation between the measured and calculated densities was smaller than 0.7 %, as shown in Figure 4.10.

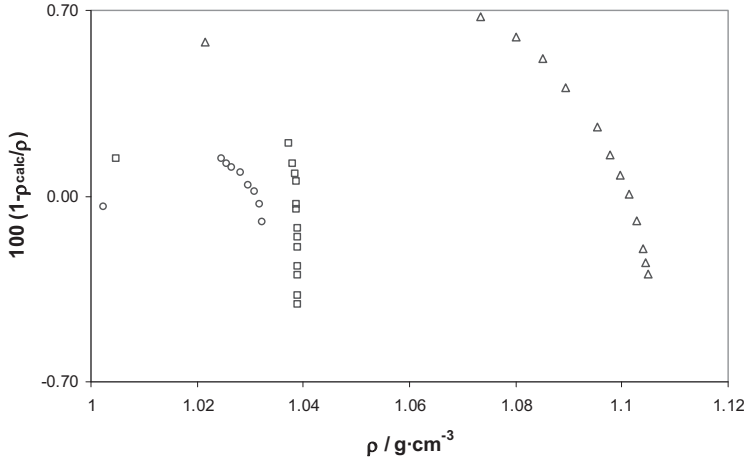

Figure 4.10 Deviation of the calculated density of carbonated aqueous solutions of DIPA from the measured density data. (○) This work, GLE static apparatus, w_3 = 10.1 % at 299.72 K ; (□) this work, GLE static apparatus, w_3 = 11.0 % at 298.22 K; (Δ) this work, GLE static apparatus, w_3 = 33.9 % at 298.29 K.

The solubility of CO_2 in water + DIPA was also measured with the bubbling apparatus at atmospheric pressure. These results are presented in [III]. Two data points from the work by Isaacs et al. [25] were measured at similar experimental conditions than those in the bubbling apparatus. The comparison against the data by Isaacs et al. [25] showed that the experimental works agreed with each other within the limits of the experimental uncertainties. The differences in amine concentration and pressure were taken into account in the comparison. Three data points measured in this work with the GLE static apparatus could be compared with the results from the bubbling apparatus. They agreed

within the limits of the experimental uncertainties, taking into account the differences in pressure and amine concentration.

The solubility of CO_2 in water + MDEA was measured with the bubbling apparatus [III]. The solubility data were compared with data at close - to - atmospheric pressure found in the literature in Figure 4.11. A numerical comparison was made with the work by Kierzkowska-Pawlak [27] and Rho et al. [30]. The maximum deviation in terms of mole fraction of CO_2 in the liquid phase was 0.0036.

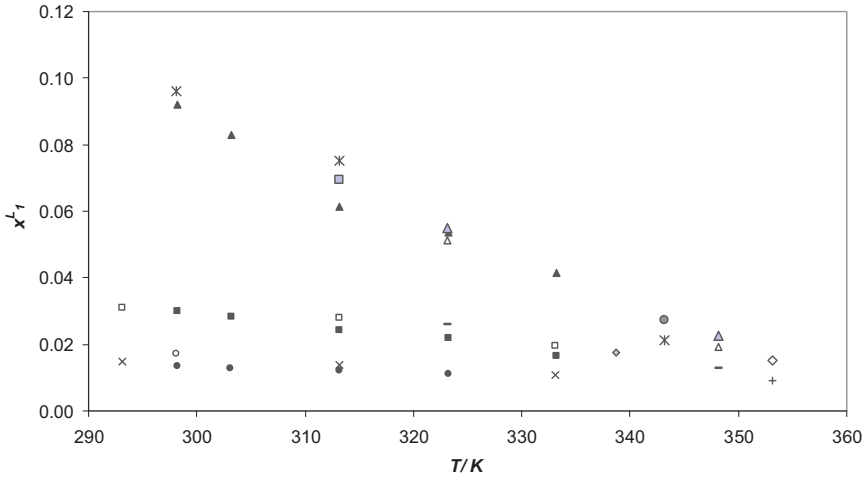

Figure 4.11 Mole fraction x_1^L of CO_2 (1) in solutions of water (2) and MDEA (3) as a function of the temperature T at atmospheric pressure. (●) This work, bubbling apparatus w_3 = 10 %; (■) this work, bubbling apparatus w_3 = 20 %; (▲) this work, bubbling apparatus w_3 = 49 %; (×) Kierzkowska-Pawlak [27] w_3 = 10 %; (○) Bhairi [28] w_3 = 11.8 %; (□) Kierzkowska-Pawlak [27] w_3 = 20 %; (+) Ermatchkov et al. [29] w_3 = 19.2 %; (◇) Bhairi [28] w_3 = 20 %; (−) Rho et al. [30] w_3 = 20.5 %; (Δ) Rho et al. [30] w_3 = 50 %; (⬭) Ma'mun et al. [31] w_3 = 50 %; (△) Park et al. [32] w_3 = 50 %; (◊) Ermatchkov et al. [29] w_3 = 48.8 %; (✳) Jou et al. [33] w_3 = 48.8 %; (▣) Austgen et al. [34] w_3 = 48.9 %.

4.4.2 Thermodynamics of water + alkanolamine systems

As listed in Table 4.1, VLE and SLE of water + DIPA and water + MDEA were measured in this work. SLE was measured by means of two experimental techniques. These results are presented in [II].

VLE data of water + DIPA at three temperatures are shown in Figure 4.12. No literature data were found for comparison. VLE data of water + MDEA were compared with

literature sources at similar conditions in [II]. The results of the numerical comparison with the work by Xu et al. [42] showed agreement within the experimental uncertainties. Kuwairi [39] developed two correlations for the vapour pressure of 1N and 2N aqueous solutions of MDEA. These correlations predicted lower vapour pressures than those measured in this work and by Sandall et al. [43].

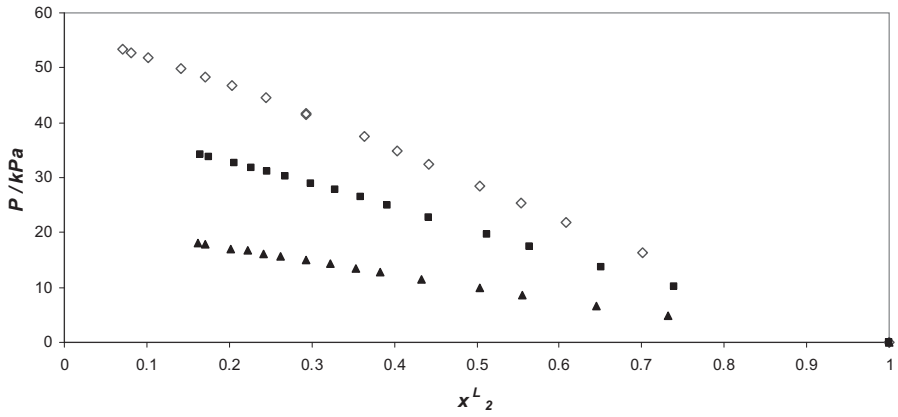

Figure 4.12 Vapour-liquid equilibrium data of the system water (1) + DIPA (2). (◊) This work, 357 K; (■) this work, 349 K; (▲) this work, 335 K.

SLE of water + DIPA was measured at low amines concentrations with a DSC, and with the visual method. The SLE measurements were possible only up to $x_2^L = 0.08$. For higher amines concentrations either the phase transition was indiscernible (visual method), or the results were of difficult interpretation (DSC). The SLE data are shown in [II]. No literature SLE data were found; therefore only the melting point of pure DIPA, measured with both techniques, was compared with literature values [112-114]. The values measured in this work, as well as the values in the literature, were scattered in a range of 4 K. The value measured with the visual method agreed with [113], while the value measured with the DSC agreed with [114].

The enthalpy of fusion of pure DIPA was measured with the DSC ($\Delta H_{fus} = 22.74$ kJ/mol). No measured values of this quantity were found in the literature. For comparison purposes, the enthalpy of fusion of pure DIPA was estimated with predicted methods, i.e. the method of Marrero and Gani [115], the method of Bondi [116] (found in [85]), and

another predicted value from [113]. The method by Marrero and Gani [115] gave the best predictions with respect to our measured value. The absolute deviation of the prediction with the method of Marrero and Gani [115] was 2.12 kJ/mol, well within the uncertainty of the estimation method (17 %).

The SLE data of water + MDEA measured with the visual method and the DSC are shown in Figure 4.13. Chang et al. [35] measured the SLE of this system. Subsequently the publication of [II], Loldrup Fosboel et al. [44] also published SLE data for water + MDEA. The literature data are included in Figure 4.13 for comparison. The SLE was measured with the visual method up to $x_2 = 0.09$, and with the DSC up to $x_2 = 0.13$. Similar problems to those encountered with DIPA also limited the measurements of the system of water + MDEA. The results of the visual method agreed with the literature data within the experimental uncertainty. The data from the DSC agreed with the other sources for $x_2 < 0.09$. At higher amine concentrations, the measured melting points were lower than expected; thus suggesting a complex SLE behaviour of the water + MDEA system. This observation was also supported by the change in aspect of the solid phase observed during the experiments with the visual method.

The phase transition of pure MDEA was indiscernible with the visual method, but the melting point was measured with the DSC. The value measured in this work agreed within the experimental uncertainty with the value found in the literature [85]. The measurements of the enthalpy of fusion of pure MDEA were unsuccessful neither such data were found in the literature.

A comparison of the SLE experimental methods suggests that the simple and inexpensive visual apparatus is suitable for SLE measurements for the purpose of modelling activity coefficients, i.e. measurements of diluted aqueous solutions of amines. In fact, when the mole fraction of amine was smaller than 0.1 the visual method gave as good results as the DSC. If measurements on a wider composition range are desired, DSC should be used.

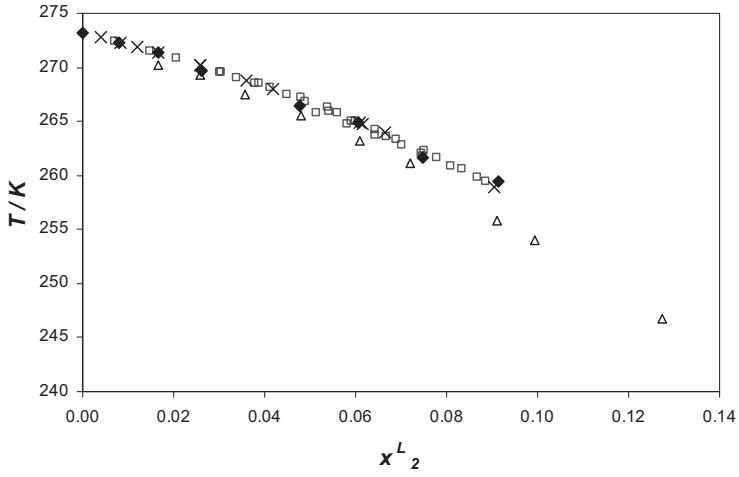

Figure 4.13 Solid-liquid equilibrium of water (1) + MDEA (2). (♦) This work, visual method; (Δ) this work, DSC; (□) Chang et al. [35]; (×) Loldrup Fosboel et al. [44].

The activity coefficients of aqueous DIPA and MDEA were modelled with the NRTL model. The model parameters were regressed using VLE, SLE and excess enthalpy data either measured in this work, or found in the open literature. All data were weighted equally during the regressions. The objective function applied in this work for VLE data is given in Eq. 4.1, where N_P is the total number of VLE data utilized in the regression. For SLE data, the objective function used the activity coefficient of water (component 1) as shown in Eq. 4.2 .The objective function for excess enthalpy data was Eq. 4.3.

Eq. 4.1
$$obj = \sum_{l=1}^{N_P} \left(\frac{P_l^{calc} - P_l^{\exp}}{P_l^{\exp}} \right)^2$$

Eq. 4.2
$$obj = \sum_{l=1}^{N_P} \left(\frac{\gamma_{1,l}^{calc} - \gamma_{1,l}^{\exp}}{\gamma_{1,l}^{\exp}} \right)^2$$

Eq. 4.3
$$obj = \sum_{l=1}^{N_P} \left(\frac{H_l^{EX,calc} - H_l^{EX,\exp}}{H_l^{EX,\exp}} \right)^2$$

The activity coefficients of water + DIPA were modelled using only the VLE and SLE data measured in this work, since no ether data were available in the literature. Long and Yamin [38] published in the journal of their university parameters of the NRTL model for

water + DIPA. They claimed that they measured the VLE of this system, but these data are not tabulated in the article. Nevertheless, the model by Long and Yamin [38] was compared with the model developed in this work [II].

The activity coefficients of water + MDEA were modelled by means of the NRTL equations using the VLE and SLE data measured in this work in addition to VLE [39-43], SLE [35]and excess enthalpy data [46,117,118] found in the literature. Details of the model are given in [II]. The activity coefficients of both aqueous alkanolamine systems are shown in Figure 4.14 at 333.15 K. The activity coefficients of water + MDEA calculated from models found in the literature [35,46-48] were also added to Figure 4.14.

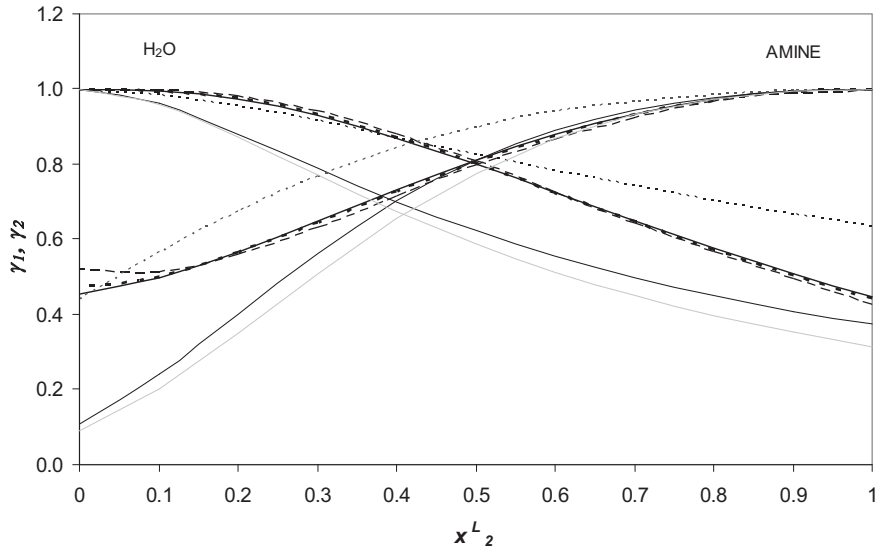

Figure 4.14 Comparison of the activity coefficients of water (1) + MDEA (2) calculated in this work by fitting VLE, SLE and excess enthalpy data with the models found in the literature at 333.15 K. (▬) This work; (– –) Posey [46];(—) Chang et al. [35]; (▪▪) Schmidt at al. [47]; (- - -) Hessen et al. [48]. Activity coefficients of the system of water (1) + DIPA (2) calculated with the NRTL model obtained by fitting VLE and SLE data at 333.15 K. (—) This work.

The models developed in this work for both aqueous alkanolamine systems always predicted monotonically decreasing activity coefficients of the amine with decreasing amine concentrations. The models found in the literature for water + MDEA, instead, predicted an increase in the activity coefficient of MDEA at low amine concentrations.

This phenomenon becomes more evident while increasing the temperature, as shown in Figure 4.15 at 393.15 K. It should be noticed that this temperature is still within the range of validity of the models parameters. The behaviour of the activity coefficient of MDEA at low amine concentrations influences the shape of the Gibbs energy, as shown in Figure 4.16. Our model predicted the common parabolic shape of the Gibbs energy, while the other models predicted more complex shapes.

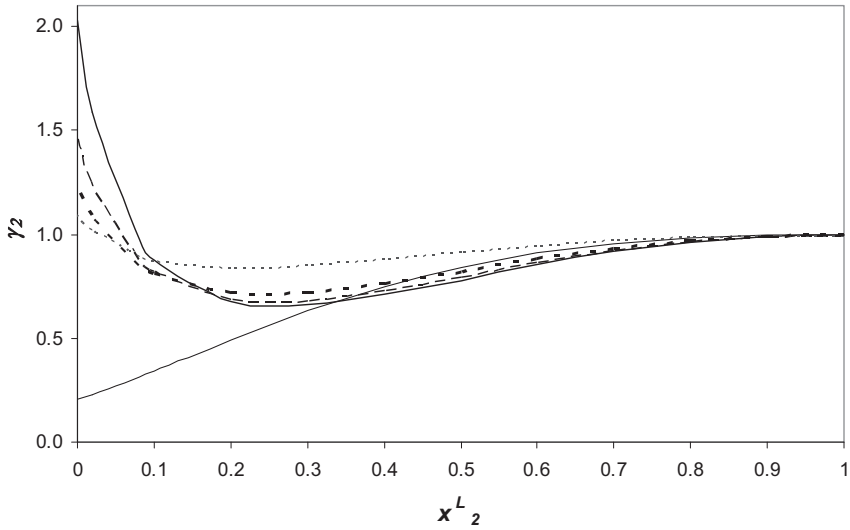

Figure 4.15 Comparison of the activity coefficients of water (1) + MDEA (2) calculated in this work by fitting VLE, SLE and excess enthalpy data with the models found in the literature at 393.15 K. (—) This work; (– –) Posey [46];(—) Chang et al. [35]; (▪▪) Schmidt et al. [47]; (- - -) Hessen et al. [48].

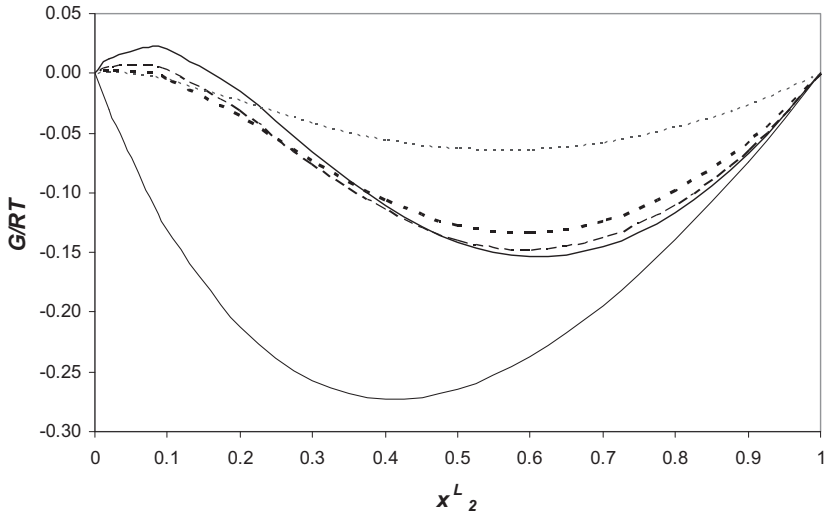

Figure 4.16 Comparison of the Gibbs energy of water (1) + MDEA (2) calculated in this work with the models found in the literature at 393.15 K. (▬) This work; (– –) Posey [46];(—) Chang et al. [35]; (▪▪) Schmidt at al. [47]; (- - -) Hessen et al. [48].

With respect to performances, the model of water + MDEA developed in this work improved the predictions in pressure (in terms of absolute pressure residual), and obtained equally good predictions of the activity coefficients of water as all the other models. With respect to excess enthalpy, only the model by Schmidt et al. [47] gave slightly better predictions.

Experimental infinite dilution excess enthalpy data were also found in the literature [46, 118, 119]. A comparison in terms of partial excess enthalpy at infinite dilution of MDEA, and of infinite dilution activity coefficients is presented in [II].

4.4.3 Henry's law constant of CO_2 in aqueous alkanolamine solutions

A model of the Henry's law constant of CO_2 in aqueous alkanolamine solutions was developed in [I]. CO_2 absorption in aqueous alkanolamine solutions is mainly the result of chemical reactions; thus it is difficult to measure directly the Henry's law constant of CO_2 in these solvents. Due to the similarities between CO_2 and N_2O, Clarke [120] introduced the so-called N_2O analogy, by which it is possible to calculate the Henry's law constant of CO_2 in aqueous alkanolamine solutions (S) from the Henry's law constant of

N_2O in the same solvent (Eq. 4.4). N_2O does not react with alkanolamine solvents, so its Henry's constant can be directly measured. The problem of modelling the Henry's law constant of CO_2 in aqueous alkanolamine solutions thus reduces to modelling the Henry's law constant of N_2O in aqueous alkanolamine solutions.

Eq. 4.4 $$H_{CO_2,S} = H_{N_2O,S}\left(\frac{H_{CO_2,W}}{H_{N_2O,W}}\right)$$

According to Eq. 4.4, expressions of the Henry's law constant of CO_2 and N_2O in water (W) are needed. The solubility of CO_2 in water was modelled according to the work by Carroll et al. [91], whose correlation also agreed with our solubility measurements, as shown in [III]. The solubility of N_2O in water was modelled using data from literature sources, as described in [I].

The Henry's law constant of a gas in a mixed solvent may be calculated, as a first approximation, from the Henry's law constant of the pure components by means of the ideal solution mixing rule [1]. The ideal model can be improved by taking into account an excess term for the Henry's constant. A new expression of the excess Henry's law constant of N_2O in aqueous binary and ternary alkanolamine solutions was developed in this work as a function of temperature and solvent composition. The parameters of the new expression were fitted using experimental Henry's law constant data points up to 120 ºC, thus reaching industrial gas-sweetening operative temperatures (e.g. regeneration in a MEA plant usually takes place at 100- 120ºC [121]). The binary solvents were aqueous solutions of MEA, DEA, DIPA, MDEA and AMP, while the ternary solvents were aqueous blends of MDEA + MEA, + DEA, + DIPA or + AMP, and AMP + MEA or + DEA. The model may be applied to any binary or ternary aqueous amine solvent, as long as Henry's constant binary solvent measurements are available for parameter regression.

The expression of the Henry's law constant of N_2O in a binary alkanolamine solvent is expressed in Eq. 4.5 as the sum of an ideal term and an excess term. The Henry's law constant of N_2O in a ternary alkanolamine solvent is shown in Eq. 4.6. In the model equations water is component 1, the amines are components 2 and 3. The liquid mole fractions refer to the unloaded solvent.

Eq. 4.5 $$H_{N_2O,12} = \sum_{i=1}^{2} H_{N_2O,i} x_i^L + H_{N_2O,12}^{EX} = \sum_{i=1}^{2} H_{N_2O,i} x_i^L + A_{12}\left[x_1^L x_2^L\right]^2 \left[1 - \frac{T}{B_{12}}\right] \exp\left[-C_{12} x_2^L\right]$$

Eq. 4.6 $$H_{N_2O,123} = \sum_{i=1}^{3} H_{N_2O,i} x_i^L + A_{123}\left[x_1^L \left(\sum_{i=2}^{3} x_i^L\right)\right]^2 \left[1 - \frac{T}{B_{123}}\right] \exp\left[-C_{123}\left(\sum_{i=2}^{3} x_i^L\right)\right] + \frac{D_{23} x_2^L x_3^L}{\left(x_2^L + x_3^L\right)^2}$$

The model empirical parameters are symmetrical. Parameters A_{ij}, B_{ij} and C_{ij} were regressed using 648 experimental Henry's law constant points in binary solvents. Parameters D_{ij} were obtained from 316 Henry's law constant measurement points in ternary solvents. The ternary parameter A_{ijk}, B_{ijk} and C_{ijk} were calculated using mixing rules from the binary parameters. The detailed model equations and the experimental data used in the regression of the parameters are given in [I]. A comparison between the model prediction and the experimental data is shown in Figure 4.17 for the system of N_2O + water + DIPA. The average absolute residual of the Henry's law constant for this system was 3.4 %. The model predictions for N_2O in water + DIPA + MDEA are shown in Figure 4.18. The average absolute residual of the Henry's law constant for this system was 2.6%.

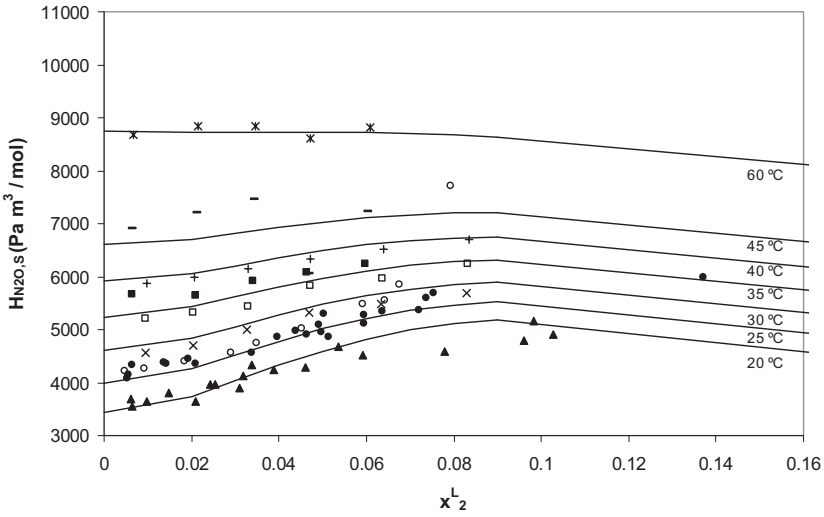

Figure 4.17 Henry's law constant of N_2O in aqueous solutions of DIPA (2). Comparison between the model developed in this work and experimental data. (——) This work (20, 25, 30, 35, 40, 45, 60 ºC); (▲) Versteeg et al. [53] at 20 ºC; (●) Versteeg et al. [53] at 25 ºC; (■) Versteeg et al. [53] at 35 ºC; (-) Versteeg et al. [53] at 45 ºC; (∗) Versteeg et al. [53] at 60 ºC; (○) Sada et al. [122] at 25 ºC; (×) Tsai et al. [123] at 30 ºC; (□) Tsai et al. [123] at 35 ºC; (+) Tsai et al. [123] at 40 ºC. The mole fractions refer to the unloaded solvent.

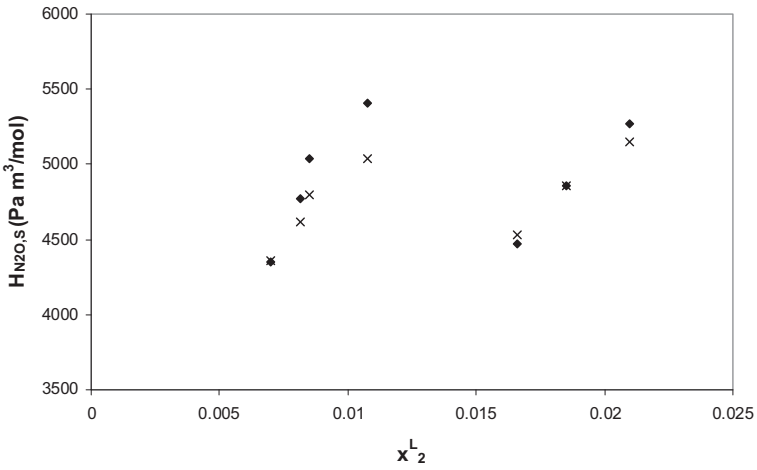

Figure 4.18 Henry's law constant of N_2O in water (1) + DIPA (2) + MDEA (3). Comparison between the predictions of the model developed in this work and experimental data. (♦) Littel et al. [124] at 25 ºC (various amount of DIPA and MDEA); (×) This work at 25 ºC. The same compositions as in Littel et al. [124] were used. The mole fractions refer to the unloaded solvent.

Other Henry's law constant models were found in the literature for various alkanolamine systems [49-55]. Most of these models, similarly to the model developed in this work, combine thermodynamic principles and empirical parameters usually determined from physical solubility measurements. Wang et al. [49] and Li and Mather [51] developed a model for the solubility of N_2O in water + DIPA. Versteeg et al. [53] proposed for the same system a composition-dependent polynomial expression of the Henry's law constant at 5 temperatures (20, 25, 35, 45, 60 ºC). The models from the literature were compared against the model developed in this work in Figure 4.19.

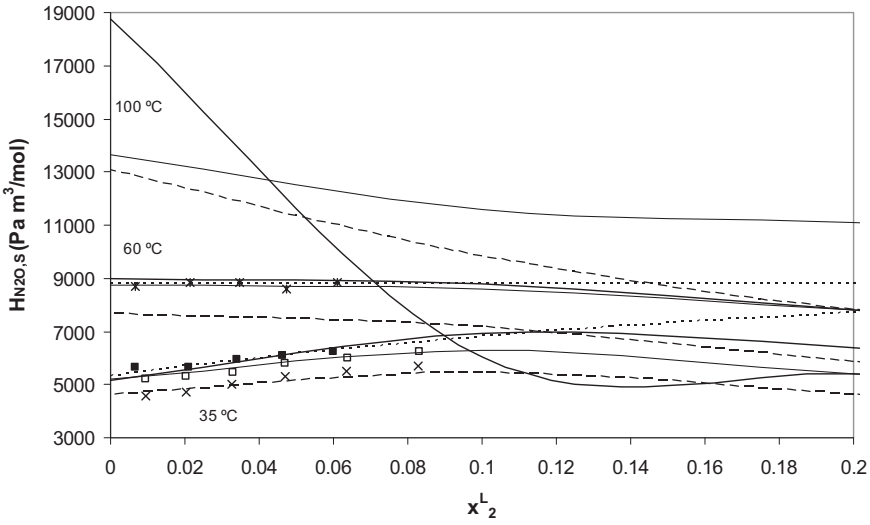

Figure 4.19 Henry's law constant of N_2O in aqueous solutions of DIPA (2). Comparison of the model developed in this work with other models found in the literature. (▬)This work (35, 60, 100 ºC); (—) Wang et al. [49](35, 60, 100 ºC); (- -) Li and Mather [51] (35, 60, 100 ºC); (···) Versteeg et al. [53] (35, 60 ºC); (■) Versteeg et al. [53] at 35 ºC; (∗) Versteeg et al. [53] at 60 ºC; (×) Tsai et al. [123] at 30 ºC; (□) Tsai et al. [123] at 35 ºC. The mole fractions refer to the unloaded solvent.

The polynomials by Versteeg et al. [53] describe well the data points measured by the authors, and used in the regression of the parameters. As mentioned above, the polynomials are isothermal, thus this model can only be calculated at the given temperatures. The model by Li and Mather [51] gives good results for the experimental

data at 35 ºC, but underestimates the Henry's law constant at 60 ºC. The authors were uncertain about the reasons of the poor performances of their model at temperatures above 45 ºC for aqueous solutions of DIPA. They suggested it may depend on the lack of density data of water + DIPA solutions at high temperatures, which was true when their model was published [51]. The model by Wang et al. [49] represents well the experimental data at 35 and 60 ºC, but when extrapolated to higher temperatures (100 ºC) it predicts a rather improbable behaviour of the Henry's law constant. The model developed in this work behaves consistently with the lower temperatures and with the other amine systems even when extrapolated up to higher temperatures. The average absolute residual of the Henry's law constant calculated on 82 measured point was 3.4 % for our model, 3.8 % for the model by Wang et al. [49], and 8.1 % for Li and Mather [51]. Graphical and numerical comparisons among the models for all the systems studied in this work are given in [I].

In general, this semiempirical model predicts the Henry's law constant of N_2O in binary and ternary aqueous amine solvents either comparably or better than the literature models. It is particularly successful in describing ternary solvent systems, improving the performances of the literature models even when D_{23} is set equal to zero, i.e. the ternary solvent is predicted based solely on binary solvent data. Additional features of the model are mathematical simplicity and consistent behaviour on the whole composition, and temperature range (i.e. up to 120 ºC) [I].

5 Conclusions

An accurate representation of the phase separation may be sufficient to design full scale separation plants, such as distillation columns. The aim of this research was to strengthen modelling of separation processes of industrial interest by improving the thermodynamic representation of the equilibrium between phases. This was successfully achieved in this work through targeted experimental investigations and thermodynamic modelling of chosen systems.

Several experimental methods were developed in this work to measure VLE, GLE and SLE data. A total of 135 VLE data points were measured for binary systems of butane + alcohol, which are important in the field of biofuels and in the production of gasoline additives. Some of these systems also presented azeoptropic behaviour, and our data contributed to the determination of the azeotropic point. Mixtures of sulphur compounds and hydrocarbons are often encountered in refinery applications, but data in the open literature are extremely scarce. This shortage negatively influenced the prediction of sulphur compounds behaviour in refinery separation units. Therefore, phase equilibrium data of sulphur compounds are greatly needed. This work supplied 129 VLE datapoints of binary systems of diethyl sulphide in C_4 – hydrocarbons. It was found that traditional activity coefficients models satisfactorily predicted most of the systems studied. In average, activity coefficient models with empirical parameters predicted the thermodynamic behaviour of the system studied better than predictive model, thus confirming the importance of experimental phase equilibrium data for thermodynamic modelling.

In this work great attention was given to CO_2 both for its role in industrial applications and as a greenhouse gas. CO_2 removal with alkanolamine solutions is a process of industrial importance in refinery, and CO_2 capture applications. A scarcity of experimental data was noticed for some alkanolamine systems, and in particular for aqueous solutions of DIPA. Before the publications of this work, neither a model for the solubility of CO_2 in DIPA solvents, nor a satisfactory thermodynamic model of aqueous DIPA solutions was available. CO_2 solubility in aqueous DIPA solvents, VLE and SLE data of DIPA solutions were measured. The first activity coefficient model for aqueous

DIPA solution based on VLE and SLE data was developed in this work. Alongside DIPA, also aqueous solutions of MDEA were modelled, due to their importance in carbon capture applications. CO_2 solubility in aqueous MDEA, VLE and SLE data of MDEA solutions were measured. The activity coefficient model for aqueous MDEA solutions developed in this work predicts better than the models found in the literature for the same system.

It was noticed that many of the existing models of the Henry's law constant of CO_2 in solutions of alkanolamines highly deviated from the experimental data at temperatures closed to the industrial. This was recognised as an important source of error in modelling the solubility of CO_2 in solutions of alkanolamines. Therefore, a new model for the Henry's law constant of CO_2 binary and ternary aqueous solutions of alkanolamines was developed. The new model is mathematically simple and reliable up to high temperatures, where most of the other models failed. In particular, this model was better than any other model in predicting ternary aqueous solvent systems, even when predictions were solely based on binary solvent data.

In future work, the large amount of experimental data and modelling work accomplished in this research may be unified into a full thermodynamic model for the solubility of CO_2 in aqueous alkanolamine solutions. Other researchers already used our published data in developing their solubility model, thus confirming the importance of these measurements in the field of alkanolamine technology. While developing the full solubility model of CO_2 in aqueous alkanolamine solutions, chemical reactions should also be addressed due to the high reactivity of these systems. This strong thermodynamic framework will be the base for successful modelling of absorption and regeneration units both in refinery applications and in carbon capture.

References

[1] H. C. Van Ness, M. M. Abbott, Classical thermodynamics of nonelectrolyte solutions with applications to phase equilibria, McGraw-Hill, New York, 1982.

[2] R. A. Meyers, Handbook of Petroleum Refining Processes (3rd Edition), McGraw-Hill, USA, 2004.

[3] T. M. Soria, F. A. Sanchez, S. Pereda, S. B. Bottini. Fluid Phase Equilib. 296 (2010) 116-124.

[4] X. Courtial, C. Soo, C. Coquelet, P. Paricaud, D. Ramjugernath, D. Richon. Fluid Phase Equilib. 277 (2009) 152-161.

[5] C. B. Kretschmer, R. Wiebe. J. Am. Chem. Soc. 74 (1952) 1276-1277.

[6] L. B. Petty, J. M. Smith. Ind. Eng. Chem. 47 (1955) 1258-1265.

[7] V. N. Churkin, V. A. Gorshkov, S. Y. Pavlov, E. N. Levicheva, L. L. Karpacheva. Zh. Fiz. Khim. 52 (1978) 488-489.

[8] K. Fischer, S. J. Park, J. Gmehling. ELDATA: Int. Electron. J. Phys. Chem. Data. 2 (1996) 135-148.

[9] A. D. Leu, D. B. Robinson, S. Y. K. Chung, C. J. Chen. Can. J. Chem. Eng. 70 (1992) 330-334.

[10] A. D. Leu, C. J. Chen, D. B. Robinson. AIChE Symp. Ser. 85 (1989) 11-16.

[11] P. Moilanen, P. Uusi-Kyyny, J. Pokki, M. Pakkanen, J. Aittamaa. J. Chem. Eng. Data. 53 (2008) 83-88.

[12] A. Deak, A. I. Victorov, T. W. de Loos. Fluid Phase Equilib. 107 (1995) 277-301.

[13] T. Anyu, X. Xianjin, S. Yuguang. Chengdu Keji Daxue Xuebao. 4 (1992) 19-25.

[14] F. W. Melpolder. Fluid Phase Equilib. 26 (1986) 279-288.

[15] S. Brunet, D. Mey, G. Perot, C. Bouchy, F. Diehl. Appl. Catal., A. 278 (2005) 143-172.

[16] P. O. Vistisen, P. Zeuthen. Ind. Eng. Chem. Res. 47 (2008) 8471-8477.

[17] W. H. Hoffert, K. Wendtner. J. Inst. Pet. 35 (1949) 171-192.

[18] E. Sapei, P. Uusi-Kyyny, K. I. Keskinen, J. Pokki, V. Alopaeus. Fluid Phase Equilib. 301 (2011) 200-205.

[19] E. Sapei, A. Zaytseva, P. Uusi-Kyyny, K. I. Keskinen, J. Aittamaa. Fluid Phase Equilib. 252 (2007) 130-136.

[20] E. Sapei, A. Zaytseva, P. Uusi-Kyyny, K. I. Keskinen, J. Aittamaa. J. Chem. Eng. Data. 52 (2007) 571-576.

[21] E. Sapei, A. Zaytseva, P. Uusi-Kyyny, K. I. Keskinen, J. Aittamaa. J. Chem. Eng. Data. 52 (2007) 192-198.

[22] The petroleum handbook, 4th ed., Shell International Petroleum, London, 1959.

[23] A. L. Kohl, R. B. Nielsen, Gas Purification (5th Edition), Elsevier 1997.

[24] Z. Bensetiti, I. Iliuta, F. Larachi, B. P. A. Grandjean. Ind. Eng. Chem. Res. 38 (1999) 328-332.

[25] E. E. Isaacs, F. D. Otto, A. E. Mather. J. Chem. Eng. Data. 22 (1977) 71-73.

[26] H. ter Maat, S. Praveen, P. Ijben, D. Arslan, H. F. Wouters, P. J. G. Huttenhuis, J. A. Hogendoorn, G. F. Versteeg, The determination of VLE data on CO2 and H2S in MDEA and its blends with other amines. Research report 186, Gas Processor Association, Tulsa, 2004.

[27] H. Kierzkowska-Pawlak. Sep. Sci. Technol. 42 (2007) 2723-2737.

[28] A. M. Bhairi, Experimental equilibrium between acid gas and ethanolamine solutions. Ph.D. Thesis. Oklaoma State University, Stillwater, 1984.

[29] V. Ermatchkov, A. Perez-Salado Kamps, G. Maurer. Ind. Eng. Chem. Res. 45 (2006) 6081-6091.

[30] S. Rho, K. Yoo, J. S. Lee, S. C. Nam, J. E. Son, B. Min. J. Chem. Eng. Data. 42 (1997) 1161-1164.

[31] S. Ma'mun, R. Nilsen, H. F. Svendsen, O. Juliussen. J. Chem. Eng. Data. 50 (2005) 630-634.

[32] M. K. Park, O. C. Sandall. J. Chem. Eng. Data. 46 (2001) 166-168.

[33] F. Y. Jou, A. E. Mather, F. D. Otto. Ind. Eng. Chem. Process Des. Dev. 21 (1982) 539-544.

[34] D. M. Austgen, G. T. Rochelle, C. C. Chen. Ind. Eng. Chem. Res. 30 (1991) 543-555.

[35] H. T. Chang, M. Posey, G. T. Rochelle. Ind. Eng. Chem. Res. 32 (1993) 2324-2335.

[36] H. Renon, J. M. Prausnitz. AIChE J. 14 (1968) 135-144.

[37] S. M. Walas, Phase equilibria in chemical engineering, Butterworths, Boston, MA, 1985.

[38] F. Long, Z. Yamin. J. Nanjing Univ. Chem. Technol. 2 (2001) 45-48.

[39] B. S. Kuwairi, Vapor pressure of selected pure materials and mixtures. Ph.D. Thesis. Oklaoma State University, USA, 1983.

[40] R. Sidi-Boumedine, S. Horstmann, K. Fischer, E. Provost, W. Furst, J. Gmehling. Fluid Phase Equilib. 218 (2004) 85-94.

[41] G. Kuranov, B. Rumpf, N. A. Smirnova, G. Maurer. Ind. Eng. Chem. Res. 35 (1996) 1959-1966.

[42] S. Xu, S. Qing, Z. Zhen, C. Zhang, J. J. Carroll. Fluid Phase Equilib. 67 (1991) 197-201.

[43] O. C. Sandall, E. B. Rinker, S. Ashour, Acid Gas Treating by Aqueous Alkanolamines. GRI Annual Report. (1993).

[44] P. L. Fosboel, M. G. Pedersen, K. Thomsen. J. Chem. Eng. Data. 56 (2011) 995-1000.

[45] D. M. Austgen, A model for Vapor-Liquid Equilibria for acid gas-alkanolamine-water systems. PhD. Thesis. University of Texas, Austin, USA, 1989.

[46] M. L. Posey, Thermodynamic model for acid gas loaded aqueous alkanolamine solutions. PhD. Thesis. University of Texas, Austin, USA, 1996.

[47] K. A. G. Schmidt, Y. Maham, A. E. Mather. J. Therm. Anal. Calorim. 89 (2007) 61-72.

[48] E. T. Hessen, T. Haug-Warberg, H. F. Svendsen. Chem. Eng. Sci. 65 (2010) 3638-3648.

[49] Y. W. Wang, S. Xu, F. D. Otto, A. E. Mather. Chem. Eng. J. 48 (1992) 31-40.

[50] H. A. Al-Ghawas, D. P. Hagewiesche, G. Ruiz-Ibanez, O. C. Sandall. J. Chem. Eng. Data. 34 (1989) 385-391.

[51] Y. Li, A. E. Mather. Fluid Phase Equilib. 96 (1994) 119-142.

[52] Y. Zhang, C. Chen. Ind. Eng. Chem. Res. 50 (2011) 163-175.

[53] G. F. Versteeg, W. P. M. Van Swaaij. J. Chem. Eng. Data. 33 (1988) 29-34.

[54] Y. Liu, L. Zhang, S. Watanasiri. Ind. Eng. Chem. Res. 38 (1999) 2080-2090.

[55] A. Jamal, Absorption and desorption of CO2 and CO in alkanolamine systems. Ph.D. Thesis. The University of British Columbia, Canada., 2002.

[56] L. Zong, C. Chen. Fluid Phase Equilib. 306 (2011) 190-203.

[57] J. M. Prausnitz, R. N. Lichtenhaler, E. G. d. Azevedo, Molecular thermodynamics of fluid-phase equilibria, 2nd ed., Prentice-Hall, Englewood Cliffs, NJ, 1986.

[58] S. I. Sandler, Chemical and engineering thermodynamics, 3rd ed., Wiley, New York, 1999.

[59] H. G. Rackett. J. Chem. Eng. Data. 15 (1970) 514-517.

[60] A. Jakob, R. Joh, C. Rose, J. Gmehling. Fluid Phase Equilib. 113 (1995) 117-126.

[61] G. Soave. Chem. Eng. Sci. 27 (1972) 1197-1203.

[62] O. Redlich, J. N. S. Kwong. Chem. Rev. 44 (1949) 233-244.

[63] G. M. Wilson. J. Am. Chem. Soc. 86 (1964) 127-130.

[64] D. S. Abrams, J. M. Prausnitz. AIChE J. 21 (1975) 116-128.

[65] A. Fredenslund, R. L. Jones, J. M. Prausnitz. AIChE J. 21 (1975) 1086-1099.

[66] U. Weidlich, J. Gmehling. Ind. Eng. Chem. Res. 26 (1987) 1372-1381.

[67] R. Wittig, J. Lohmann, J. Gmehling. Ind. Eng. Chem. Res. 42 (2003) 183-188.

[68] J. Gmehling, R. Wittig, J. Lohmann, R. Joh. Ind. Eng. Chem. Res. 41 (2002) 1678-1688.

[69] A. Klamt, F. Eckert. Fluid Phase Equilib. 172 (2000) 43-72.

[70] S. Lin, S. I. Sandler. Ind. Eng. Chem. Res. 41 (2002) 899-913.

[71] F. A. Mato, R. B. Mato, F. Mato. Ind. Eng. Chem. Res. 28 (1989) 1441-1446.

[72] P. L. Fosboel, K. Thomsen, E. H. Stenby. Ind Eng Chem Res. 48 (2009) 4565-4578.

[73] C. C. Chen, H. I. Britt, J. F. Boston, L. B. Evans. AIChE J. 28 (1982) 588-596.

[74] C. C. Chen, L. B. Evans. AIChE J. 32 (1986) 444-454.

[75] B. Mock, L. B. Evans, C. C. Chen. AIChE J. 32 (1986) 1655-1664.

[76] C. Chen, Y. Song. AIChE J. 50 (2004) 1928-1941.

[77] C. Chen, Y. Song. Ind. Eng. Chem. Res. 43 (2004) 8354-8362.

[78] C. Chen, Y. Song. Ind. Eng. Chem. Res. 44 (2005) 8909-8921.

[79] G. M. Bollas, C. C. Chen, P. I. Barton. AIChE J. 54 (2008) 1608-1624.

[80] D. M. Austgen, G. T. Rochelle, X. Peng, C. C. Chen. Ind. Eng. Chem. Res. 28 (1989) 1060-1073.

[81] K. S. Pitzer. J. Am. Chem. Soc. 102 (1980) 2902-2906.

[82] A. A. Rashin, B. Honig. J. Phys. Chem. 89 (1985) 5588-5593.

[83] P. Uusi-Kyyny, J. Pokki, M. Laakkonen, J. Aittamaa, S. Liukkonen. Fluid Phase Equilib. 201 (2002) 343-358.

[84] J. A. Barker. Aust. J. Chem. 6 (1953) 207-210.

[85] DIPPR, Project 801- Full version 2005/2008/2009. Design institute for physical property data/AIChE.

[86] I. M. A. Fonseca, J. P. B. Almeida, H. C. Fachada. J. Chem. Thermodyn. 39 (2007) 1407-1411.

[87] M. A. Postigo, M. Katz. J. Solution Chem. 16 (1987) 1015-1024.

[88] P. Kruus, C. A. Hayes. Can. J. Chem. 63 (1985) 3403-3410.

[89] A. H. Harvey. AIChE J. 42 (1996) 1491-1494.

[90] R. Crovetto. J. Phys. Chem. Ref. Data. 20 (1991) 575-589.

[91] J. J. Carroll, J. D. Slupsky, A. E. Mather. J. Phys. Chem. Ref. Data. 20 (1991) 1201-1209.

[92] E. Wilhelm, R. Battino, R. J. Wilcock. Chem. Rev. 77 (1977) 219-262.

[93] I. R. Krichevsky, J. S. Kasarnovsky. J. Am. Chem. Soc. 57 (1935) 2168-2171.

[94] R. H. Loeppert, V. Dohnal, Methods of Soil Analysis, Part 3. Chemical Method. SSSA Book Series No. 5, in: Sparks DL (Ed.), Madison, WI, 1996.

[95] S. Hovorka, V. Dohnal. J. Chem. Eng. Data. 42 (1997) 924-933.

[96] J. R. Taylor, An introduction to error analysis: the study of uncertainties in physical measurements, 2nd ed., University Science Books, Sausalito (CA), 1997.

[97] W. V. Wilding, N. F. Giles, L. C. Wilson. J. Chem. Eng. Data. 41 (1996) 1239-1251.

[98] N. A. Darwish, Z. A. Al-Anber. Fluid Phase Equilib. 131 (1997) 287-295.

[99] K. Fischer, J. Gmehling. J. Chem. Eng. Data. 39 (1994) 309-315.

[100] C. Christensen, J. Gmehling, P. Rasmussen, U. Weidlich, T. Holderbaum, Heats of Mixing Data Collection. DECHEMA Chemistry Data Series, Volume III. Part 1, Frankfurt/Main, 1984.

[101] P. Uusi-Kyyny, J. Pokki, J. Aittamaa, S. Liukkonen. J. Chem. Eng. Data. 46 (2001) 1244-1248.

[102] Y. Kim, J. Pokki, K. Rehak, J. Matous, J. Aittamaa. J. Chem. Eng. Data. 49 (2004) 246-250.

[103] T. Ouni, P. Uusi-Kyyny, J. Pokki, J. Aittamaa. J. Chem. Eng. Data. 49 (2004) 787-794.

[104] J. Pokki, M. Laakkonen, P. Uusi-Kyyny, J. Aittamaa. Fluid Phase Equilib. 212 (2003) 129-141.

[105] A. Zaytseva, P. Uusi-Kyyny, J. Pokki, M. Pakkanen, J. Aittamaa. J. Chem. Eng. Data. 49 (2004) 1168-1174.

[106] H. Laavi, P. Uusi-Kyyny, J. Pokki, M. Pakkanen, V. Alopaeus. J. Chem. Eng. Data. 53 (2008) 913-918.

[107] C. L. Yaws. Chemical Properties Handbook. McGraw-Hill, New York, 1999.

[108] R. H. Perry, D. W. Green, Perry's Chemical Engineers' Handbook. 7th ed., McGraw-Hill, New York, 1997.

[109] R. C. Reid, J. M. Prausnitz, B. E. Poling, The Properties of Gases and Liquids. 4th ed., McGraw-Hill, New York, 1987.

[110] A. Henni, J. J. Hromek, P. Tontiwachwuthikul, A. Chakma. J. Chem. Eng. Data. 48 (2003) 1062-1067.

[111] R. H. Weiland, J. C. Dingman, D. B. Cronin, G. J. Browning. J. Chem. Eng. Data. 43 (1998) 378-382.

[112] Handbook of Fine Chemicals, Aldrich Chemical Co., Milwaukee, WI, 1988-1989.

[113] The Alkanolamines Handbook, Dow Chemical Company, Midland, Michigan, 1981.

[114] M. J. Astle, R. C. Weast, Handbook of Data on Organic Compounds, CRC Press Inc., Boca Raton, FL., 1985.

[115] J. Marrero, R. Gani. Fluid Phase Equilib. 183-184 (2001) 183-208.

[116] A. Bondi. Chem. Rev. 67 (1967) 565-580.

[117] Y. Maham, A. E. Mather, C. Mathonat. J. Chem. Thermodyn. 32 (2000) 229-236.

[118] Y. Maham, A. E. Mather, L. G. Hepler. J. Chem. Eng. Data. 42 (1997) 988-992.

[119] J. H. Kim, C. Dobrogowska, L. G. Hepler. Can. J. Chem. 65 (1987) 1726-1728.

[120] J. K. A. Clarke. Ind. Eng. Chem. Fundam. 3 (1964) 239-245.

[121] M. S. Jassim, G. T. Rochelle. Ind. Eng. Chem. Res. 45 (2006) 2465-2472.

[122] E. Sada, H. Kumazawa, M. A. Butt. J. Chem. Eng. Data. 23 (1978) 161-163.

[123] T. Tsai, J. Ko, H. Wang, C. Lin, M. Li. J. Chem. Eng. Data. 45 (2000) 341-347.

[124] R. J. Littel, G. F. Versteeg, W. P. M. Van Swaaij. J. Chem. Eng. Data. 37 (1992) 49-55.

Errata Corrige

Publication III. Chapter 2.2.4 pg. 104.

The sentence: ”The Poynting correction of CO2 was calculated with the Krichevsky–Kasarnovsky correction [10]” should be removed.

The Krichevsky–Kasarnovsky GLE equation was not used in this work, since the activity coefficient of the solute CO_2 was not assumed equal to unity. The activity coefficient and the Poynting correction of water were assumed equal to unity.

The purpose of this research was to develop modelling of industrial processes by improving the thermodynamic representation of the equilibrium between phases. For this purpose an extensive experimental work was performed. Vapour liquid equilibrium of binary mixtures of butane + alcohols and of diethyl sulphide + C4 – hydrocarbons were studied. Absorption of carbon dioxide in alkanolamine solutions is the leading industrial technology for the removal of carbon dioxide. In recent years, this technology has gained importance also for carbon capture from large point sources. The scarcity of experimental data for some alkanolamine systems affected the accuracy of thermodynamic models. Several experimental techniques were developed in this work to supply new data for the solubility of carbon dioxide in aqueous solutions of diisopropanolamine (DIPA) and methyldiethanolamine (MDEA). The vapour-liquid equilibrium and the solid-liquid equilibrium of aqueous DIPA and MDEA were also studied and modelled.

Aalto-DD 20/2012

ISBN 978-952-60-4518-4
ISBN 978-952-60-4519-1 (pdf)
ISSN-L 1799-4934
ISSN 1799-4934
ISSN 1799-4942 (pdf)

Aalto University
School of Chemical Technology
Department of Biotechnology and Chemical Technology
www.aalto.fi

BUSINESS + ECONOMY

ART + DESIGN + ARCHITECTURE

SCIENCE + TECHNOLOGY

CROSSOVER

DOCTORAL DISSERTATIONS